



Published in final edited form as:

*J Med Chem.* 2021 September 09; 64(17): 12790–12807. doi:10.1021/acs.jmedchem.1c00837.

## 1,3-Diarylpyrazolyl-acylsulfonamides as potent anti-tuberculosis agents targeting cell wall biosynthesis in *Mycobacterium tuberculosis*

Lutete Peguy Khonde<sup>a</sup>, Rudolf Müller<sup>a</sup>, Grant A. Boyle<sup>a</sup>, Virsinha Reddy<sup>a</sup>, Aloysius T. Nchinda<sup>a</sup>, Charles J. Eyermann<sup>a</sup>, Stephen Fienberg<sup>a</sup>, Vinayak Singh<sup>b,c</sup>, Alissa Myrick<sup>b,#</sup>, Efrem Abay<sup>d</sup>, Mathew Njoroge<sup>d</sup>, Nina Lawrence<sup>d</sup>, Qin Su<sup>e</sup>, Timothy G Myers<sup>e</sup>, Helena I. M. Boshoff<sup>f</sup>, Clifton E. Barry III<sup>f</sup>, Frederick A Sirgel<sup>g</sup>, Paul D van Helden<sup>g</sup>, Lisa M. Massoudi<sup>h</sup>, Gregory T. Robertson<sup>h</sup>, Anne J. Lenaerts<sup>h</sup>, Gregory S. Basarab<sup>a,d</sup>, Sandeep R. Ghorpade<sup>a,\*</sup>, Kelly Chibale<sup>a,c,\*</sup>

<sup>a</sup>Drug Discovery and Development Centre (H3D), Department of Chemistry, University of Cape Town, Rondebosch 7701, South Africa

<sup>b</sup>Drug Discovery and Development Centre (H3D), Institute of Infectious Disease and Molecular Medicine, University of Cape Town, Rondebosch 7701, South Africa

<sup>c</sup>South African Medical Research Council Drug Discovery and Development Research Unit, Department of Chemistry and Institute of Infectious Disease and Molecular Medicine, University of Cape Town, Rondebosch 7701, South Africa

<sup>d</sup>Drug Discovery and Development Centre (H3D), Division of Clinical Pharmacology, Department of Medicine, University of Cape Town, Observatory, 7925, South Africa

<sup>e</sup>Genomic Technologies Section, Research Technologies Branch, National Institute of Allergy and Infectious Diseases, National Institutes of Health, Bethesda, Maryland 20892, United States

\*Corresponding Authors Phone: +27 21 650 2553. kelly.chibale@uct.ac.za, Phone: +27 21 650 1250. Sandeep.ghorpade@uct.ac.za.  
#AM deceased in November 2019.

### Author Contributions

Chemical synthesis, compound design and SAR expansion was led by R.M. Chemical synthesis was performed by R.M., L.P.K., G.A.B., V.R., A.T.N. Computational and compound design support was provided by C.J.E. Pharmacophore model was developed and written by S.F. Analysis and interpretation of the biology data was done by V.S. and A.M. *In vivo* PK experiments were performed by E.A. MetID studies were performed by M.N. *In vitro* DMPK data was analyzed by N.L. Agilent microarray protocols were developed by Q.S. and T.G.M. The screening of DuPont compound library and RNA microarray experiment were performed by H.I.M.B. MIC data was generated by H.I.M.B. High-throughput screening was conceptualized and led by C.E.B. MICs against clinical isolates were conducted by F.A.S. and P.D.v.H. Efficacy studies were planned and conducted by L.M. and G.R. Efficacy studies were guided by A.L. G.S.B. provided scientific and strategic guidance for the work and edited the manuscript. S.R.G. provided strategic support and gave inputs on compound design. Introduction, hit identification, SAR, biology triage, conclusion sections of the manuscript were written by S.R.G. Synthesis and chemistry experimental sections were written by L.P.K. *In vitro* and *in vivo* DMPK, efficacy section were written by M.N. and S.R.G. and were further edited by G.R. Funding acquisition by K.C. along with scientific and strategic support. All authors have given approval to the final version of the manuscript.

The authors declare no competing financial interest.

### ASSOCIATED CONTENT

The Supporting Information is available free of charge on the ACS Publications website.

Synthetic schemes, Synthesis of intermediates, Analytical spectra for lead compounds, microbiology assays, *in vitro* DMPK assays, mouse pharmacokinetic studies, *In vivo* efficacy studies (PDF)

Data from RNA microarray experiment (XLS)

Molecular formula strings and some data (CSV)

<sup>f</sup>Tuberculosis Research Section, Laboratory of Clinical Infectious Diseases; National Institute of Allergy and Infectious Diseases, National Institutes of Health, Bethesda, Maryland 20892, United States

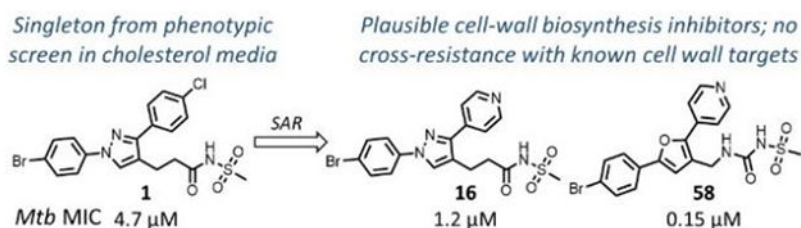
<sup>g</sup>South African Medical Research Council Centre for Tuberculosis Research / DST/NRF Centre of Excellence for Biomedical Tuberculosis Research, Division of Molecular Biology and Human Genetics, Faculty of Medicine and Health Science, Stellenbosch University, Tygerberg, Cape Town, 7505, South Africa

<sup>h</sup>Mycobacteria Research Laboratories, Department of Microbiology, Immunology, and Pathology, Colorado State University, Fort Collins, Colorado 80523, United States

## Abstract

Phenotypic whole cell high-throughput screening of a ~150,000 diverse set of compounds against *Mycobacterium tuberculosis* (*Mtb*) in cholesterol-containing media identified 1,3-diarylpyrazolyl-acylsulfonamide **1** as a moderately active hit. Structure-activity relationship (SAR) studies demonstrated a clear scope to improve whole cell potency to MIC values of <0.5  $\mu\text{M}$  and a plausible pharmacophore model was developed to describe the chemical space of active compounds. Compounds are bactericidal *in vitro* against replicating *Mtb* and retained activity against multidrug resistant clinical isolates. Initial biology triage assays indicated cell wall biosynthesis as a plausible mode-of-action for the series. However, no cross-resistance with known cell wall targets such as MmpL3, DprE1, InhA and EthA was detected suggesting a potentially novel mode-of-action or inhibition. The *in vitro* and *in vivo* drug metabolism and pharmacokinetics profiles of several active compounds from the series were established leading to the identification of a compound for *in vivo* efficacy proof-of-concept studies.

## Graphical Abstract



## Keywords

Tuberculosis; *Mycobacterium tuberculosis*; Phenotypic screen; TB Drug Discovery; 1,3-Diarylpyrazolyl acylsulfonamides

## INTRODUCTION

Tuberculosis (TB) continues to be a global epidemic most severely affecting the underprivileged sectors of society throughout the world. According to the World Health Organization (WHO) 2019 global TB report, 10 million people fell sick with TB in 2018 and 1.5 million people lost their lives.<sup>1</sup> The most common drug regimen currently

used for the treatment of drug-sensitive TB is 40-years old and consists of four drugs - rifampicin (RIF), isoniazid (INH), pyrazinamide (PZA) and ethambutol (EMB) - taken over a minimum period of six months. The long treatment duration along with unpleasant side-effects often leads to patient non-compliance, resulting in the development of drug resistant TB, *viz.* multidrug resistant (MDR) TB that is refractory to two frontline drugs RIF and INH and the extensively drug resistant (XDR) TB that develops additional resistance to any fluoroquinolone and at least one of the three injectable second-line drugs (amikacin, kanamycin, or capreomycin). Treatments for drug-resistant TB are fraught with limited choices of poorly efficacious medicines with severe side-effects and lengthy treatment durations of 18–24 months. Hence, there has been a strong global drive towards identifying safe new drugs with novel mode-of-actions (MoAs), which would be effective for treatment of drug-resistant TB and be included in combination regimens aimed at treatment shortening for drug-sensitive TB. Gratifyingly, a few recently approved drugs with novel MoAs such as bedaquiline,<sup>2</sup> pretomanid,<sup>3</sup> and delamanid<sup>4</sup> have been added to the arsenal of the available TB drugs. Several follow-up drug candidates such as the DprE1 inhibitors Macozinone (MCZ, PBTZ-169)<sup>5</sup> and TBA-7371,<sup>6</sup> MmpL3 inhibitor SQ-109,<sup>7</sup> QcrB inhibitor Telacebec (Q203)<sup>8</sup> and the Leucyl-tRNA synthetase inhibitor GSK 3036656<sup>9</sup> are in the clinical development pipeline (Fig. 1). Other known drugs such as linezolid have also shown great promise in the treatment of MDR-TB and have encouraged pre-clinical efforts to discover safer analogues.<sup>10</sup> Considering the significant attrition rates in clinical development and empirical nature of effective combination therapy toward shorter treatments, there is a continuous need to replenish the global TB drug pipeline with new bactericidal agents that avoid pre-existing clinical drug resistance, either through novel MoA or novel mode-of-inhibition (MoI) of clinically validated drug targets.

*Mycobacterium tuberculosis* (*Mtb*), the causative agent of TB, is known to adapt metabolically to the various nutrients available during its cycle of infection, persistence, and reactivation.<sup>11, 12</sup> Fatty acids and cholesterol are important carbon sources for *in vivo* survival and pathogenesis of *Mtb*<sup>13, 14</sup> even though this organism can utilize carbohydrates and carbon dioxide as carbon sources and needs glucose for *in vivo* persistence.<sup>15</sup> There have been efforts to screen compound libraries against *Mtb* surviving on fatty acid and cholesterol media to identify compounds efficacious against various pathological forms of *Mtb*.<sup>16</sup> Herein we report structure-activity relationship (SAR) studies and preliminary target identification studies of 1,3-diarylpyrazolyl-acylsulfonamides identified from the phenotypic screening of a compound library supplied by DuPont in cholesterol-containing media.

## Results and Discussion.

### Phenotypic hit with a novel mode-of-action.

A high-throughput phenotypic whole cell screen of a ~150,000 diverse set of compounds from a DuPont Agrichemicals compound library against *Mtb* was conducted at the National Institute of Allergy and Infectious Diseases of the National Institutes of Health (NIAID/NIH, U.S.) using *Mtb* in two different media, Middlebrook 7H9/DPPC/cholesterol/BSA/Tyloxapol (DPPC/chol) and Middlebrook 7H9/butyrate pH 6.0 /nitrite/BSA/Tyloxapol (butyrate pH6/nitrite). This screen identified ~2000 primary hits. The activity of these

hits was confirmed by determining the minimum inhibitory concentrations (MICs) that lead to no visible growth from solid samples against *Mtb* under three conditions - DPPC/ chol, and butyrate pH6/nitrite as well as 7H9/DPPC/casitone/Tyloxapol (DPPC/cas). Of the three media used, activity in DPPC/chol medium may closely simulate *in vivo* nutritional ambience for replicating *Mtb* whereas DPPC/cas is a protein-free minimal media used to identify weaker inhibitors that would be missed in standard serum containing media due to the effect of protein-binding. The low pH butyrate medium containing nitrite reflects some of the environmental stresses encountered by *Mtb* residing in macrophages *in vivo*, namely – acidic pH of the intraphagosomal environment of the macrophage and reactive nitrite intermediates (RNI) released from nitrite.<sup>14, 17</sup> Among the few hits that confirmed from the screening campaign, compound **1** was identified as a singleton with moderate activity under the various media conditions; notably it did not show any previous literature reports of antitubercular activity (Table 1). Though **1** has a 1,3-diarylpyrazole core found in some known anti-*Mtb* actives,<sup>18, 19</sup> it has a unique *N*-(methylsulfonyl)propanamide substituent at the pyrazole C4 position. It had been reported as a potassium channel modulator for the treatment of a variety of human disorders.<sup>20</sup> Screening against various tool strains of *Mtb* indicated a novel MoA as described in the biology triage section of this manuscript. The compound was non-cytotoxic against HepG2 cell-line under both glucose and galactose containing media conditions at the highest concentration tested, minimizing the possibility of mitochondrial cytotoxicity.<sup>21</sup> All these observations sparked further interest in exploring the potential of **1** to deliver a novel drug candidate for TB treatment. Detailed SAR and target identification studies were initiated as detailed in the following sections.

## Synthesis.

As the hit compound **1** was identified as a singleton from the screen, detailed SAR studies were needed to identify key pharmacophoric features and to expand the SAR scope for increasing anti-*Mtb* activity. To this end a systematic exploration of each substituent around the central pyrazole ring and variations of the pyrazole core were undertaken. Compounds were specifically synthesized to explore the SAR around substituents around the N1 (compounds **1–12**, Table 2), C3 (compounds **13–25**, Table 3), and C4 positions (compounds **26–45**, Table 4). Furthermore, additional compounds were synthesized to explore replacements for the *N*-(methylsulfonyl)propanamide substituent at the C4-position (compounds **46–50**, Table 5) and to vary the central pyrazole core (compounds **51–58**, Table 6).

Compound **1–25** and **35** were synthesized by modification of the reaction sequence described previously as depicted in Scheme 1.<sup>20</sup> In short, the key intermediates, 4-formylpyrazoles (**A**) were synthesized by treating the appropriately substituted hydrazones with POCl<sub>3</sub> in a Vilsmeier-Haack formylation reaction, which was followed by a regioselective Knövenagel condensation reaction with malonic acid to obtain the corresponding *trans*-acrylic acids **B**. Selective reduction of the acrylic acids in order to avoid concomitant halogen hydrogenolysis gave the corresponding propanoic acid intermediates **C** which were coupled with methanesulfonamide in the presence of CDI and DBU or, in a few cases, in the presence of DCC and DMAP to yield target compounds. The detailed synthetic schemes are described in Supplementary Information (Schemes S1 and S2). Synthesis of

compounds **26-41** with modified alkyl linkers at C4 are described in Schemes S3–S6. Urea and carbamate derivatives **42-45** could be synthesized from common intermediate **A** via alcohols **D** and amines **E** as described in Scheme S7. Synthesis of compounds **46-50** with replacement of acylsulfonamide functionality are described in Schemes S8 and S9. Synthesis of compounds **51-58** with variations to the central pyrazole core are described in Schemes S10–S14.

### SAR at the M1-substituent.

*Mtb* activity measured as MIC in Middlebrook 7H9/Glu/BSA/Tx media and aqueous solubility were monitored as first tier criteria towards selection of compounds for further characterization (Table 2). Compound **2** with an unsubstituted phenyl ring showed a much higher MIC (>50  $\mu\text{M}$ ) relative to **1**. Replacement of *p*-bromo on the phenyl ring with *p*-fluoro, as in **3**, or moving bromine to the *-meta* or *-ortho* positions as in **4** and **5**, respectively, led to deterioration of activity (MICs  $\approx$  50  $\mu\text{M}$ ). Similarly, **6** with the phenyl ring replaced with 4-pyridyl, and **7** with a cyclohexyl ring showed much weaker MICs ( $\approx$  50  $\mu\text{M}$ ). Compounds **11** and **12** with polar CN and methylsulfoxide groups respectively at the *para* position of the phenyl ring showed 5–10-fold weaker activity indicating the essentiality of hydrophobic substituents at this position. Only compounds **8** and **9** with *p*-chlorophenyl and *p*-CF<sub>3</sub>-phenyl, respectively, retained MICs similar to **1**, albeit with lower aqueous solubility (100 and 50  $\mu\text{M}$ , respectively). Compound **10** with a 4-CF<sub>3</sub>-3-pyridyl ring at M1 showed a comparable MIC to **1** with somewhat improved solubility (90  $\mu\text{M}$ ) compared to **9**. Overall, variations at the M1-phenyl ring (R<sub>1</sub>) demonstrated the essentiality of an aryl ring with larger hydrophobic para-substituents for *Mtb* activity.

### SAR at the C3-position.

Compared to the M1 position, substituents at the C3-position (R<sub>2</sub>) of the pyrazole showed a wider scope for structural variation leading to slightly lower MICs (Table 3). Compound **13** with a hydrogen atom in place of Cl on the C3 phenyl group retained a similar MIC to **1**. Compound **14** with *m*-Cl-phenyl also retained a similar MIC, but compound **15** with *o*-Cl-phenyl showed a >10-fold higher MIC. Compound **16** with a 4-pyridyl ring at C3 in place of Cl-phenyl improved the MIC  $\sim$ 4-fold, thus providing a more potent tool compound for MoA studies (see below). Compound **17** with a 3-pyridyl ring showed a MIC similar to compound **1**, and **18** with a pyrazine ring showed a 5-fold higher MIC. Compounds **19** and **20** with saturated cyclohexyl and tetrahydropyran rings, respectively, at the C3-position showed MICs similar to **1**, but **21** with a basic piperidine at C3 and its *N*-formyl derivative **22** showed much weaker activity (MICs  $\approx$  50  $\mu\text{M}$ ) indicating an intolerance towards polar functionality at this position for non-aromatic R<sub>2</sub> substituents. Similarly, higher (3–5-fold) MICs were observed with **23** having a *p*-NO<sub>2</sub>-phenyl at the C3-position and the corresponding aniline derivative **24**. Compound **25** with a C3-benzyl group also showed much weaker MIC, thus limiting the SAR scope to explore directly attached aryl, heteroaryl and saturated rings.

### SAR at C4 *N*-(methylsulfonyl)propanamide.

A few analogues were synthesized to determine the essentiality of the *N*-sulfonylpropanamide functionality linked to the pyrazole C4 position (R<sub>3</sub>, Table 4). The corresponding carboxylic acid **26** and *N*-methyl amide derivative **27** showed much weaker activity (MICs >50 μM) establishing the *N*-sulfonylpropanamide as a critical functionality for potency. Methylation of the sulfonamide NH led to **28** that showed a significant decrease in activity (MIC >50 μM) along with low aqueous solubility (<5 μM). Replacement of the carbonyl group with methylene (compound **29**) led to a high MIC (>50 μM). The data points to the need for an acidic functionality (the sulfonylpropanamide) that has specific binding interaction with the target not seen with the carboxylic acid of **26**. The specificity of the sulfonylpropanamide was further supported by swapping positions of the sulfonyl and carbonyl groups (compound **30**) leading to high MICs (>50 μM). The length of alkyl chain linking the *N*-(methylsulfonyl)carbamoyl group to the pyrazole core was also critical to maintain lower MICs as demonstrated with **31** (MIC >50 μM) and **32** (MIC 37 μM) having shorter and longer linking alkyl chains to the pyrazole C4 position. The ethyl sulfonyl analogue **33** showed a 4-fold higher MIC, while the larger cyclopropylsulfonyl group was even less active (MIC >50 μM) indicating a limited scope around the sulfonyl alkyl group. Hence, the *N*-(methylsulfonyl)propanamide represents an optimal pharmacophore predicted to engage in key interactions with the target as delineated later.

Modifications on the propanamide chain were then explored to better understand SAR and continue compound optimization, particularly to improve metabolic stability of the acylsulfonamide while maintaining the potency of the compounds (refer DMPK section). Addition of a methyl group either on α- or β-carbons of the propanamide chain led to compounds **36** and **37** with much weaker activity (MICs ~50 μM) compared to the unsubstituted analogue **35** (MICs 6.25 μM) indicating a likely clash at the target level or perturbation of the preferred side chain binding conformation. Comparatively better MICs were observed by constraining the methyl group into a cyclopropane ring as in **40** and **41** (MICs 12.5–19 μM). The *trans*-acrylamide derivatives **38** and **39** showed more potent MICs (1.2–4.7 μM). Compounds **42**, **43** and **44** with a sulfonylurea tethered to C4 and a net replacement of CH<sub>2</sub> with NH showed lower MICs compared to the corresponding *N*-(methylsulfonyl)propanamide derivatives indicating a possible H-bond donor interaction from the urea NH with the target. Compound **45** with a sulfonylcarbamate functionality showed an 8-fold higher MIC relative to **43**, supporting the hypothesis that there is a contribution to binding by the urea NH.

Further, we explored replacing the *N*-acylsulfonamide group with other functionality envisioned to similarly position an acidic group. (Table 5). Compound **46** and **47** with tetrazole and 1,2,4-oxadiazolone moieties attached to C4 *via* an ethyl linker and compound **48** with a pyrimidinetrione attached *via* a methylene linker showed much higher MICs (>50 μM). Only **49** with an 1,3,4-oxadiazolone attached *via* an ethyl linker at the C4-position showed a lower MIC, about 4-fold higher than **1**, albeit the low solubility (<5 μM) rendered the compound less interesting. Overall, there is a limited scope for replacement of the *N*-acylsulfonamide functionality. Compound **50** wherein the propanamide was cyclized into a dihydroisoxazole ring also retained an MIC within 4-fold of compound **1**. Further scope

for optimization of MICs using C4-functionalities as in compounds **49** and **50** by varying other substituents in the molecule remains to be explored.

### SAR of the pyrazole core.

Table 6 shows the analogues synthesized to understand the importance of the relative positions of substituents on the pyrazole ring and the influence of alternative isosteric heterocycles. Compounds **51** and **52** retained the same relative position of all three substituents and the pyrazole nitrogen lone pair of **1** and **3** and, not surprisingly showed similar MICs. Analogues **53** and **54** with 1,4-diarylpyrazole and 3,5-diarylpyrazole cores also display the three substituents in the same relative orientation as **1** but shift the position of the pyrazole nitrogen lone pair resulting in much higher MICs (  $50 \mu\text{M}$ ) and indicating an important target interaction for the pyrazole N2 of **1**. 1,5-Diarylpyrazole **55** had a much higher MIC (  $50 \mu\text{M}$ ), further confirming the importance of relative positions of aryl rings in maintaining potency. Replacement of the pyrazole with other 5-membered heterocycles as with **56** and **57** having oxazole and thiazole cores, respectively, showed 5–8-fold weaker MICs. Compound **58** with a furan core showed much more potent activity with MIC below  $0.5 \mu\text{M}$ . The above observations indicate a smaller angle between the R1 and R2 substituents on the smaller pyrazole and furan heterocycles ( $150.3^\circ$  and  $125.5^\circ$  respectively) are favored over what would be seen with the larger thiazole core ( $154.6^\circ$ ) in **57**. Loss of potency for oxazole **56** is consistent with the observation that polar atoms are not well tolerated at other position of 5-membered ring as seen for **53** and **54**. The furan oxygen is favorable as is the 2-position N of the pyrazole of **1** and of **51**. Improved activity of furan analogue **58** could be attributed to O being more electronegative than N, possibly making a stronger hydrogen bonding interaction with the target.

The above SAR demonstrates the specific structural requirements of compound **1** and analogues required to maintain anti-*Mtb* activity alluding to specific target engagement by the scaffold.

### Representative Pharmacophore.

We have accordingly developed a pharmacophore hypothesis to summarize key structural features of the scaffold that may aid in efforts to further optimize this series. To describe the chemical space of the active acyl sulfonamide pyrazole compounds, a series of pharmacophore hypotheses were generated from the set of compounds using the Phase module from the Schrodinger molecular modelling suite.<sup>22</sup> The activity cutoff was defined as MIC  $< 25 \mu\text{M}$  in the 7H9/glucose/BSA/Tx assay among the set of 58 compounds in this series. An AARRR (A- acceptor, R – ring) pharmacophore hypothesis (Fig. 2) consisting of three aromatic rings (R, R<sub>1</sub> and R<sub>2</sub>), and two hydrogen bond acceptors was found to best describe the chemical space of active compounds. A central aromatic ring feature (R) corresponds to the central pyrazole core with two more aromatic ring features corresponding to aromatic substitutions at the 1 and 3 positions (R<sub>1</sub> and R<sub>2</sub> respectively). The first acceptor feature (A<sub>1</sub>) can be found approximately  $5.65 \text{ \AA}$  from the C4-position of the pyrazole core fitting the negatively charged N of the acyl sulfonamide moiety. At physiological pH, the acyl sulfonamide NH is deprotonated, creating an anion that could serve as a hydrogen bond acceptor. The second acceptor (A<sub>2</sub>) lies another  $2.43 \text{ \AA}$  away forming a  $158^\circ$  angle between

A<sub>1</sub> and the central ring feature (Fig. 2A). A<sub>1</sub> moves out of the plane formed by the three ring features forming a 95 ° dihedral angle around a line connecting the R feature and the A<sub>1</sub> feature (Fig. 2B). In this set of compounds, R<sub>1</sub> often seems, at a minimum, to require negatively charged acid groups as only compounds with a pK<sub>a</sub> below physiological pH have shown activity.

A representative active compound **43** fits all five of these features very closely (Fig. 3A). The pharmacophore fit of each ligand was determined via Phase docking with the fit evaluated using Phase fitness score.<sup>22</sup> All active compounds featured in this manuscript fit the five features (Fig. 3B) very closely.

A bioisostere replacement of the acyl sulfonamide with the 1,3,4-oxadiazolone of **49** introduces an acid center with a predicted<sup>23</sup> pK<sub>a</sub> of 7.87 +/- 0.4, in contrast to the predicted pK<sub>a</sub> of the sulfonamide of **43** of 3.72 +/- 0.23 thus lowering the propensity for an acceptor/negative charge to form at physiological pH. Since the oxadiazolone has a pK<sub>a</sub> close to physiological pH, both the protonation and deprotonated states need to be considered. Only the deprotonated form fits all five features of the pharmacophore hypothesis. This poorer fit explains the weaker MIC (19 μM) of **49** compared to **43** (1.56 μM) (Fig. S1c).

Compounds **28–31** were all inactive with poor pharmacophore fits for at least one reason as explained in supplementary section with Figure S1. Compounds **33** and **34** (Fig. 3C) with their respective ethyl and cyclopropyl attachments to the sulfone and **36** and **37** with methyl groups in positions α and β to the pyrazole core all showed near perfect fits for the pharmacophore model despite a complete loss of activity. These compounds contain additional bulk occupying regions not defined by the pharmacophore suggesting potential excluded volumes. Excluded volumes beyond the A<sub>2</sub> feature and adjacent to the alkyl linker at the sites of potential branching would penalize these compounds. These excluded volumes would need more examples to be properly defined. An overlay of all the inactive compounds presented in the study (Fig. 3D) demonstrates many of them to occupy regions that could be considered for excluded volumes.

Compound **58** with a furan core fulfills all pharmacophore features (Fig. S1d) and showed potent activity whereas compounds **53**, **54** and **56** with changes in the core ring (R) are examples of weak actives with good fits. Comparing the matched pair of inactive **53** and active **51** would suggest that a heteroaromatic acceptor N contributes to activity. However, small changes to the π-characteristics of the core caused by these rearrangements may also contribute to the lower activity. More data from analogues containing rearrangements of this core would be needed to confirm the contribution of this acceptor and warrant expanding the definition of this pharmacophore feature to include an acceptor corresponding to the 2-position of the pyrazole core.

### Biology triage.

Compounds **1**, **8**, **43** and **58** were screened against various tool strains of *Mtb* to deconvolute the MoA for anti-*Mtb* activity. None of the compounds showed modulation in MICs against a cytochrome *bd* oxidase knockout mutant strain ( *cyd*)<sup>24, 25</sup> nor against a QcrB mutant (QcrBA317T), thereby eliminating the two targets of the respiratory pathway as a



likely target (Table 7). Neither did the compounds elicit a positive response in the *PrecA*-LUX bioluminescence reporter assay,<sup>26</sup> which is designed to detect modulation in *recA* expression, an indicator of DNA damage, hence ruling it out as a MoA for the compounds (Fig. S2 in supplementary information). However, the compounds showed sustained signals in the *PiniB*-LUX bioluminescence reporter assay that detects modulation in *iniBAC* operon expression,<sup>26</sup> an indicator of cell wall biosynthesis being disrupted (Fig. S3). The prediction that the compounds inhibited cell wall biosynthesis was further confirmed by transcriptional profiling studies that showed upregulation in the genes involved in cell wall biosynthesis including many of the genes upregulated by isoniazid (INH) including *acpM*, *fabD*, *kasA*, *kasB*, *accD6*, *rv2248*, *efpA*, *iniB*, *iniA* and *iniC* (Table S3 and S4 in supplementary information). Despite these similarities, some of the genes that are upregulated during isoniazid treatment (*ppsA*, *ppsB*, *ppsC*, *ppsD*, *ppsE* and *fbpC2*) were downregulated during exposure to compounds **8** and **16** indicating differences in transcriptional responses. The compounds were screened against the mutant strains of MmpL3 and DprE1 which are frequently encountered cell wall targets (Table 7). Two strains carrying a mutation in MmpL3 (G253E, or G758A) were not resistant, arguing against MmpL3 as the target. Similarly, three strains carrying mutations in DprE1 (Y314C, P116S, or T314H), which confer resistance to other DprE1 inhibitors, were not resistant, suggesting DprE1 is not the target. In addition, other isogenic single-drug resistant strains of known cell wall targeting drugs such as INH and ethionamide (ETH) were also not cross-resistant to the compounds (Table 7). Taken together, these data suggest a MoA that most likely involves interference with *Mtb* cell wall biogenesis in a manner that does not lead to cross resistance to other cell wall inhibitors. Studies to determine specific MoA of this series are underway.

### Bactericidal activity against clinical isolates.

The bactericidal activity of representative compounds **1**, **8** and **16** against replicating *Mtb* was evaluated through the exposure of *Mtb* cultures to various concentrations of compounds for 8 days and allowing the treated cultures to regrow on a fresh media after washing out the excess free drug (Fig. S4 in supplementary information). All the tested compounds showed 2–2.5 log CFU reduction at 1–4X MIC concentrations within 8 days indicating the bactericidal nature of the compounds. But the compounds were not active against non-replicating *Mtb* under nutrient starvation conditions. Compound **16** retained activity against 3 drug-sensitive, two mono-drug resistant and three MDR/XDR clinical isolates of *Mtb* indicating potential utility of the compounds from the series to treat drug-sensitive as well as drug-resistant TB (Table 8). The MIGIT (Mycobacteria Growth Indicator Tube) assay uses higher inoculum in liquid broth designed for faster growth of mycobacteria and involves longer incubation times relative to the Alamar Blue MIC microtiter plate assay used for the SAR investigation herein.<sup>27</sup> Hence, MIC values between the two assays will not be comparable. Nonetheless, it is gratifying that the MIC shifts between multidrug resistant and susceptible *Mtb* strains in the MIGIT assays were relatively small (less than 4-fold) thereby suggesting broader clinical utility.

### *In vitro* and *in vivo* DMPK profiles.

In general, the compounds in the series showed moderate to good metabolic stability in mouse, rat and human microsomes as presented in Table 9. The high plasma protein binding

(PPB) observed for the compounds may be attributed to high albumin binding associated with the acidic acylsulfonamide functionality along with the high degree of lipophilicity. Compound **20** showed lower protein binding presumably due to lower lipophilicity imparted by tetrahydropyran ring attached to the C3 position. The compounds in Table 9 were also profiled for *in vivo* pharmacokinetics following intravenous dosing in mice.

The hit compound **1** had a low *in vivo* mouse blood clearance ( $Cl_b$ ) and low volume of distribution ( $V_d$ ) that translated to a high *in vivo* exposure. Replacing the *N1* aryl group with a 4-CF<sub>3</sub>-3-pyridyl ring in **10**, led to a dramatic increase in clearance and consequently lower exposure. Rapid  $Cl_b$  values were also observed for **16** and **17** with 4-pyridyl and 3-pyridyl groups, respectively, at the C3 position. The rapid *in vivo* clearance of these compounds was all the more problematic due to the relatively high PPB leading to exceedingly high unbound clearance ( $CL_u$ ) values calculated by correcting  $Cl_b$  for plasma free fraction (assuming blood to plasma ratio of 1).<sup>28</sup> *In vivo* metabolite identification studies of **17** revealed that the high clearances were in part due to hydrolysis of the acylsulfonamide (data in supplementary information). Subsequent SAR exploration therefore focused on modifications that were designed to increase stability of the acylsulfonamide while maintaining the potency of the compounds. However, neither addition of a double bond to the acyl chain (**38**), nor cyclopropanation (**40**), replacement of the sulfonamide with a sulfonylurea (**43**), or sulfonylcarbamate (**45**) improved the clearances of the compounds. In addition, except for **10** which had a *N1* CF<sub>3</sub>-3-pyridyl ring, all pyridyl compounds had total clearances that exceeded hepatic blood flow in mice (90 mL/min/kg), which suggests that extra-hepatic metabolism may be a significant mechanism of clearance. The high TPSA and low logD of these pyridyl derivatives (Table 7), suggests that the compounds have low lipoidal permeability and it is therefore likely that transporter-mediated clearance was also a key contributor to the observed total clearance.<sup>29, 30</sup> This was further validated by performing *in vivo* metabolite identification studies on **43**. Following intravenous dosing of the compound in mice, only unchanged compound was detected in blood, urine, and feces, suggesting that metabolism was not a major contributor to its clearance. Compounds, **1**, **8** and **51** had high exposure on oral dosing (data not shown), with **8** in particular showing almost complete absorption (bioavailability >95%) even at high doses. This compound therefore had the best balance of *in vitro* potency and *in vivo* pharmacokinetics and was therefore selected for further *in vivo* proof-of-concept studies.

### ***In vivo* efficacy**

*In vivo* efficacy testing was performed at an oral dose of 200 mg/kg in the acute Balb/c mouse model to evaluate the ability of **8** to inhibit replicating intracellular *Mtb* in lungs.<sup>31–34</sup> Treatment was initiated 7 days after a low-dose aerosol infection with *Mtb* Erdman pFCA LuxAB strain<sup>32</sup> and continued for 12 consecutive days. The compound was well tolerated during the treatment period but was not efficacious in reducing *Mtb* lung burdens in treated mice relative to the untreated mice as measured by quantification of relative light units (RLU) of the luciferase expressing Erdman strain from lung homogenate or by CFU counts obtained by plating serial dilutions of lung homogenate on agar plates. As a positive control, EMB at 100 mg/kg once a day led to a 2-log CFU reduction in this model. To explain the results, the free oral exposure of compound **8** in healthy mice at 200 mg/kg oral dose was

compared with the MIC against the *Mtb* Erdman strain used for the efficacy studies (9.1  $\mu\text{M}$ ) and inhibitory concentration against intracellular *Mtb* ( $\text{IC}_{90} = 11 \mu\text{M}$ ) (Fig. 4). In-study PK performed on the last 2 days of treatment matched closely with the healthy PK (data in SI). From the two analyses, it is evident that compound **8** at 200 mg/kg failed to achieve drug exposures necessary to exert an antimicrobial effect *in vivo*. While much higher or more frequent dosing may provide sufficient exposure to demonstrate efficacy, the underlying data suggests that further optimisation of antibacterial activity and/or PK is required to do so at lower doses that would feasibly predict human utility. Work towards achieving these improvements is in progress and will be reported in a future manuscript.

## Conclusion.

In summary, phenotypic screening of a DuPont compound library against *Mtb* in cholesterol-containing media identified 1,3-diarylpyrazolyl-acylsulfonamide **1** as a moderately active hit with a potentially novel MoA. The SAR studies described here demonstrate a clear scope to improve the MICs of compounds to  $<0.5 \mu\text{M}$  and a plausible pharmacophore model was developed to summarize SAR of the series and describe the chemical space of active compounds. Screening of the compounds against a panel of various tool strains of *Mtb* ruled out the involvement of known mechanisms and/or targets such as DNA damage and respiration but suggested involvement of cell wall damage in the mode-of-action. RNA microarray studies of *Mtb* cultures treated with the compounds confirmed the upregulation of genes that are involved in lipid metabolism/fatty acid biosynthesis. Isogenic single-drug resistant mutant strains of MmpL3, DprE1, InhA and EthA were not cross-resistant with the compounds indicating novel MoA or perhaps an alternative mode of inhibition of the targets. The compounds are bactericidal against replicating *Mtb* and retain activity against multidrug-resistant clinical isolates of *Mtb*. These features make the series an attractive chemical matter for further target identification and drug discovery efforts to potentially identify a novel clinical candidate for treatment of TB. Further drug optimization work is needed to improve upon both the *Mtb* activity of the series and the *in vivo* PK if compounds with efficacy in TB models of infection are to be realized.

## Experimental

**MIC testing and bioluminescence reporter assay.**—MIC determinations were done as previously described.<sup>35</sup> INH was included as a positive control. Briefly, *Mtb* H37Rv (ATCC 27294) was grown in Middlebrook 7H9/Glu/BSA/Tyloxapol consisting of Middlebrook 7H9 broth base (4.7 g/L)/ bovine serum albumin fraction V (5 g/L)/ dextrose (4 g/L)/ NaCl (0.81 g/L)/ 0.05% Tyloxapol to an  $\text{OD}_{650\text{nm}}$  of 0.2 at which stage cells were diluted 1000-fold in the same medium. Compound was serially diluted in Middlebrook 7H9/Glu/BSA/Tyloxapol medium in round-bottom 96-well plates (Nunc) at 50  $\mu\text{L}$ / well followed by addition of an equal volume of diluted cell suspension. Plates were incubated in sealed bags at 37 °C and growth recorded after 1- and 2-weeks of growth using an enlarging inverted mirror. The MIC was recorded as the compound concentration that completely inhibited all visible growth. Bioluminescence reporter assays were carried out as described by Naran et al.<sup>26</sup>

**MICs against mutant strains.**—Alamar Blue fluorescence-based broth microdilution assay was used to assess MICs of compounds against *Mtb* mutant strains, as described previously.<sup>36</sup> MICs were determined after 7 days of growth in standard Middlebrook 7H9/Glycerol/ADC/Tween-80. For QcrB and *cydA* mutants, the growth measurement was monitored by OD<sub>600</sub>. MIC was defined as the concentration required to inhibit growth by 90%.

**RNA extraction and Transcriptional Profiling.**—RNA extraction from *Mtb* H37Rv (ATCC 27294) grown to an OD<sub>650</sub> of 0.2 and subsequently treated for 6 h with 1X and 10X MIC of compound or vehicle control was performed using previously described methods.<sup>37</sup> RNA was also extracted from control cultures treated for 6 h with isoniazid (2  $\mu$ M) or solvent control. RNA (4 mg) yielding an RNA integrity number (RIN) of 8 or higher as determined by the Agilent 2100 Bioanalyzer was subsequently used for fluorescent-tagged cDNA synthesis with random hexamer (4.5 mg) (Invitrogen) in a final volume of 14.5  $\mu$ L by sequential heat denaturation at 70 °C for 5 minutes, cooling on ice, addition of 5  $\mu$ L of 5 $\times$  First-Strand buffer, 1.25  $\mu$ L 0.1 M DTT, 2.5  $\mu$ L of dNTP mix (consisting of 5 mM each of dATP, dGTP, dTTP and 0.5 mM dCTP), 1  $\mu$ L of 200 U/ $\mu$ L SuperScriptIII (Invitrogen), 1  $\mu$ L of 40 U/ $\mu$ L RNaseOut, and 1  $\mu$ L of Cy3 or Cy5-dCTP (GE) with incubation at 25 °C for 5 minutes and at 48 °C for 90 minutes. RNA was removed by adding 5  $\mu$ L of 1M NaOH followed by incubation at 70 °C for 15 minutes. After neutralization with 5  $\mu$ L of 1 M HCl, fluorescent cDNA was purified on Amicon Ultra-0.5 column (Millipor) according to the manufacturer's recommendations. Fluorescent cDNA was analyzed with the Nanodrop ND-1000. Equal amounts (0.7  $\mu$ g) of Cy3- and Cy5-labeled cDNA were hybridized to the Agilent SurePrint G3 4 $\times$ 44K custom oligonucleotide microarrays (design number 021966, 021362) in the TECAN HS Pro 4800 hybridization station. Hybridization was performed using Agilent 2x Gene expression hybridization HI-RPM buffer, and 10x Blocking Reagent at 65 °C for 17 h. Arrays were washed with Agilent Gene Expression Wash Buffer 1 at room temperature and Gene Expression Wash Buffer 2 at 37 °C. Slides were dried under nitrogen gas for 3 minutes at 30 °C and imaged using an Agilent high resolution DNA microarray scanner (model G2505C) at 5  $\mu$ m resolution and 100/10% PMT dual scanning for XDR extended dynamic range. Agilent Feature Extraction software was used for image analysis.

**Pharmacophore Hypothesis generation.**—To generate the pharmacophore hypothesis, all compounds in this set were prepared using Maestro 12.4<sup>38</sup> to generate minimized 3D structures and determine the most likely protonation state at biological pH. A pharmacophore model was then developed using the Phase Develop Pharmacophore Model tool.<sup>22</sup> The pharmacophore model was created from multiple ligands with the active ligands defined by an activity cutoff of MIC < 25  $\mu$ M in the 7H9/glucose/BSA/Tx assay. The find best alignment method was chosen with the default hypothesis settings of 4 to 5 features and all the default pharmacophore features allowed. The pharmacophore hypotheses generated were then inspected and the hypothesis that best represented the dataset was selected and validated against a wider set of compounds from this series.

**DMPK.**—All protocols for *in vitro* DMPK studies and mouse PK studies are available in the supplementary document. Animal studies were conducted following guidelines and

policies as stipulated in the UCT Research Ethics Code for Use of Animals in Research and Teaching, after review and approval of the experimental protocol by the UCT Senate Animal Ethics Committee (protocol FHS-AEC 013/032).

**Chemistry.**—All commercial reagents were purchased from Sigma-Aldrich, Combi-Blocks, Enamine, or Fluorochem and were used without further purification. Solvents were used as received unless otherwise stated. Analytical thin-layer chromatography (TLC) was performed on SiO<sub>2</sub> plates on aluminium backing. Visualization was accomplished by UV irradiation at 254 and 220 nm. Flash column chromatography was performed using a Teledyne ISCO flash purification system with SiO<sub>2</sub> 60 (particle size 0.040–0.055 mm, 230–400 mesh). Purity of all final derivatives for biological testing was confirmed to be >95% as determined using an Agilent 1260 Infinity binary pump, Agilent 1260 Infinity diode array detector (DAD), Agilent 1290 Infinity column compartment, Agilent 1260 Infinity standard autosampler, and Agilent 6120 quadrupole (single) mass spectrometer, equipped with APCI and ESI multimode ionization source. Using a Kinetex Core C18 2.6 μm column (50 mm × 3 mm); mobile phase B of 0.4% acetic acid, 10 mM ammonium acetate in a 9:1 ratio of HPLC grade methanol and type 1 water, mobile phase A of 0.4% acetic acid in 10 mM ammonium acetate in HPLC grade (type 1) water, with flow rate of 0.9 mL/min, detector diode array (DAD). Or an Agilent UPLC–MS was used: Agilent Technologies 6150 quadrupole, ES ionization, coupled with an Agilent Technologies 1290 Infinity II series UPLC system Agilent 1290 series HPLC at two wavelengths 254 and 290 nm using the following conditions: Kinetex 1.7 μm Evo C18 100A, LC column 50 mm × 2.1 mm, solvent A of 0.1% (formic acid) water, solvent B of 0.1% (formic acid) acetonitrile. The structures of the intermediates and final products were confirmed by <sup>1</sup>H NMR and mass spectrometry. <sup>1</sup>H NMR spectra were recorded on a Bruker spectrometer at 300 or 400 MHz. Chemical shifts (δ) are given in ppm downfield from TMS as the internal standard. Coupling constants, *J*, are recorded in hertz (Hz). Synthesis details and data of intermediates are supplied in the Supporting Information (Section 1)

### **General sulfonamide coupling procedure for the synthesis of compounds 1–25, 27–29, 31–41, 51–57.**

**Method 1. CDI-mediated sulfonamide coupling.:** To a solution of the appropriate acid (1 equiv) in DMF was added CDI (2 equiv) and the resulting reaction mixture was stirred for 10 min at 50 °C. Then the appropriate sulfonamide (1.2 equiv) and DBU (1.2 equiv) were added, and the resulting reaction mixture was heated to 90 °C for 16–48 h. The reaction mixture was then cooled to 25 °C, water was added (30 mL) and the aqueous layer was extracted with EtOAc (3 x). The combined organic layers were dried over Na<sub>2</sub>SO<sub>4</sub> and concentrated *in vacuo*. The crude reaction mixture was purified by flash chromatography using ISCO Teledyne on 12 g RediSep Rf column and elution using a gradient of the appropriate solvent mixtures to yield the desired products.

**Method 2: DCC-mediated sulfonamide coupling.:** To the solution of the appropriate acid (1.00 equiv) and methanesulfonamide (1.20 equiv) in DMF were added DCC (2.50 equiv) and DMAP (1.50 equiv). The reaction mixture was stirred at 30 °- 40 °C for 16–48 h. The reaction mixture was quenched with water (5 mL) and pH was adjusted to 6 with 1N HCl.

The aqueous phase was extracted with EtOAc (3 x). The organic phase was washed with brine, dried over Na<sub>2</sub>SO<sub>4</sub>, and concentrated *in vacuo*. The residue was purified by silica-gel column or preparative HPLC chromatography to yield the appropriate compound.

**Method 3: Acid chloride coupling with sulfonamide.:** To a solution of appropriate sulfonamide (5 equiv) in DCM was added Et<sub>3</sub>N (5 – 10 equiv). Then the appropriate acyl chloride (1 equiv) was added at 0 °C. The mixture was stirred at 15 °C to 25 °C for 16–24 h. The mixture was poured into 1N HCl and extracted with DCM. The combined organic phase was concentrated and purified by prep-HPLC or by silica gel column chromatography.

**3-(1-(4-bromophenyl)-3-(4-chlorophenyl)-1H-pyrazol-4-yl)-N-(methylsulfonyl)propanamide (1).**

**Method 3.:** Yield: 19%. <sup>1</sup>H NMR: (400MHz, DMSO-*d*<sub>6</sub>) δ 11.92–11.73 (m, 1H), 8.49–8.36 (m, 1H), 7.88–7.78 (m, 2H), 7.78–7.64 (m, 4H), 7.60–7.49 (m, 2H), 3.21 (s, 3H), 2.98–2.85 (m, 2H), 2.70–2.58 (m, 2H). <sup>13</sup>C NMR (101 MHz, DMSO-*d*<sub>6</sub>) δ 171.8, 149.5, 138.6, 132.7, 132.4 (2C), 131.8, 129.1 (2C), 128.7 (2C), 127.8, 120.1, 119.9 (2C), 118.4, 41.0, 35.7, 19.2. LC/MS (APCI<sup>+</sup>): Calculated for C<sub>19</sub>H<sub>17</sub>BrClN<sub>3</sub>O<sub>3</sub>S 480.99; Observed *m/z* [M+H]<sup>+</sup> 482.0, 483.9; HPLC purity: >99%.

**3-(3-(4-chlorophenyl)-1-phenyl-1H-pyrazol-4-yl)-N-(methylsulfonyl)propanamide (2).**

**Method 2.:** Yield: 32%. <sup>1</sup>H NMR: (400MHz, DMSO-*d*<sub>6</sub>) δ 12.09 – 11.57 (m, 1H), 8.45 – 8.34 (m, 1H), 7.89 – 7.81 (m, 2H), 7.81 – 7.71 (m, 2H), 7.62 – 7.46 (m, 4H), 7.37 – 7.29 (m, 1H), 3.18 (s, 3H), 3.00 – 2.86 (m, 2H), 2.64 – 2.57 (m, 2H). LC/MS (APCI<sup>+</sup>): Calculated for C<sub>19</sub>H<sub>18</sub>ClN<sub>3</sub>O<sub>3</sub>S 403.08; Observed *m/z* [M+H]<sup>+</sup> 404.1; HPLC purity: >99%.

**3-(3-(4-chlorophenyl)-1-(4-fluorophenyl)-1H-pyrazol-4-yl)-N-(methylsulfonyl)propanamide (3).**

**Method 1.:** Yield: 14%. <sup>1</sup>H NMR (300 MHz, DMSO-*d*<sub>6</sub>) δ 11.72 (s, 1H), 8.36 (s, 1H), 7.91 – 7.84 (m, 2H), 7.78 – 7.71 (m, 2H), 7.59 – 7.52 (m, 2H), 7.37 (t, *J* = 8.8 Hz, 2H), 3.21 (s, 3H), 2.93 (t, *J* = 7.5 Hz, 2H), 2.63 (t, *J* = 7.5 Hz, 2H). LC/MS (ESI<sup>+</sup>): Calculated for C<sub>19</sub>H<sub>17</sub>ClFN<sub>3</sub>O<sub>3</sub>S 421.07; Observed *m/z* [M+H]<sup>+</sup> 422.1; HPLC purity: 97%.

**3-(1-(3-bromophenyl)-3-(4-chlorophenyl)-1H-pyrazol-4-yl)-N-(methylsulfonyl)propanamide (4).**

**Method 1.:** Yield: 20%. <sup>1</sup>H NMR (300 MHz, DMSO-*d*<sub>6</sub>) δ 11.72 (s, 1H), 8.48 (s, 1H), 8.09 (t, *J* = 1.9 Hz, 1H), 7.88 (dt, *J* = 7.2, 2.0 Hz, 1H), 7.81 – 7.73 (m, 2H), 7.60 – 7.43 (m, 4H), 3.21 (s, 3H), 2.93 (t, *J* = 7.5 Hz, 2H), 2.64 (t, *J* = 7.5 Hz, 2H). LC/MS (APCI<sup>+</sup>): Calculated for C<sub>19</sub>H<sub>17</sub>BrClN<sub>3</sub>O<sub>3</sub>S 480.99; Observed *m/z* [M+H]<sup>+</sup> 481.9, 483.9; HPLC purity: 97%.

**3-(1-(2-bromophenyl)-3-(4-chlorophenyl)-1H-pyrazol-4-yl)-N-(methylsulfonyl)propanamide (5).**

**Method 2.:** Yield: 31%. <sup>1</sup>H NMR (400 MHz, Chloroform-*d*) δ 7.74–7.65 (m, 5H), 7.60–7.58 (m, 3H), 7.45–7.43 (m, 1H), 3.27–3.25 (m, 3H), 3.13–3.07 (m, 2H), 2.64–2.58 (m, 2H).

LC/MS (APCI<sup>+</sup>): Calculated for C<sub>19</sub>H<sub>17</sub>BrClN<sub>3</sub>O<sub>3</sub>S 480.99; Observed *m/z* [M+H]<sup>+</sup> 482.0; 484.0; HPLC purity: >99%.

**3-(3-(4-chlorophenyl)-1-(pyridin-4-yl)-1*H*-pyrazol-4-yl)-*N*-(methylsulfonyl)propanamide (6).**

**Method 2.:** Yield: 23%. <sup>1</sup>H NMR (400MHz, DMSO-*d*<sub>6</sub>) δ 8.67–8.62 (m, 2H), 8.62–8.57 (m, 1H), 8.22–8.14 (m, 1H), 7.89–7.85 (m, 2H), 7.81–7.76 (m, 2H), 7.60–7.55 (m, 2H), 3.00–2.97 (m, 3H), 2.90–2.86 (m, 2H); <sup>1</sup>H NMR (400MHz, DMSO-*d*<sub>6</sub> + D<sub>2</sub>O) δ 8.64–8.56 (m, 2H), 8.51–8.45 (m, 1H), 8.29–8.12 (m, 1H), 7.86–7.79 (m, 2H), 7.78–7.68 (m, 2H), 7.58–7.50 (m, 2H), 3.03 (s, 3H), 2.90–2.81 (m, 2H). LC/MS (APCI<sup>+</sup>): Calculated for C<sub>18</sub>H<sub>17</sub>ClN<sub>4</sub>O<sub>3</sub>S 404.07; Observed *m/z* [M+H]<sup>+</sup> 405.0; HPLC purity: 98%.

**3-(3-(4-chlorophenyl)-1-cyclohexyl-1*H*-pyrazol-4-yl)-*N*-(methylsulfonyl)propanamide (7).**

**Method 2.:** Yield: 37%. <sup>1</sup>H NMR (400 MHz, Chloroform-*d*) δ 7.74 (s, 1H), 7.57–7.55 (m, 2H), 7.42–7.40 (m, 2H), 7.35 (s, 1H), 4.14–4.10 (m, 1H), 3.26 (s, 3H), 3.04–3.00 (t, *J* = 7.2 Hz, 2H), 2.54–2.51 (t, *J* = 7.2 Hz, 2H), 2.20–2.17 (m, 2H), 1.94–1.91 (m, 2H), 1.77–1.71 (m, 3H), 1.46–1.26 (m, 3H). LC/MS (APCI<sup>+</sup>): Calculated for C<sub>19</sub>H<sub>24</sub>ClN<sub>3</sub>O<sub>3</sub>S 409.12; Observed *m/z* [M+H]<sup>+</sup> 410.0; HPLC purity: 96%.

**3-(1,3-bis(4-chlorophenyl)-1*H*-pyrazol-5-yl)-*N*-(methylsulfonyl)propanamide (8).**

**Method 1.:** Yield: 52%. <sup>1</sup>H NMR (300 MHz, Methanol-*d*<sub>4</sub>) δ 8.14 (s, 1H), 7.84 – 7.75 (m, 2H), 7.76 – 7.66 (m, 2H), 7.54 – 7.46 (m, 4H), 3.21 (s, 3H), 3.10 – 2.98 (m, 2H), 2.64 (t, *J* = 7.4 Hz, 2H). <sup>13</sup>C NMR (151 MHz, Methanol-*d*<sub>4</sub>) δ 174.0, 151.9, 140.0, 135.1, 133.3, 132.9, 130.6 (2C), 130.5 (2C), 129.8 (2C), 129.0 (2C), 121.3 (2C), 41.4, 37.4, 20.4. LC/MS (ESI<sup>+</sup>): Calculated for C<sub>19</sub>H<sub>17</sub>Cl<sub>2</sub>N<sub>3</sub>O<sub>3</sub>S 437.04; Observed *m/z* [M+H]<sup>+</sup> 438.1; HPLC purity: >99%.

**3-(3-(4-chlorophenyl)-1-(4-(trifluoromethyl)phenyl)-1*H*-pyrazol-4-yl)-*N*-(methylsulfonyl)propanamide (9).**

**Method 3.:** Yield: 11%. <sup>1</sup>H NMR (400 MHz, Chloroform-*d*) 7.92 (s, 1H), 7.85–7.83 (d, *J* = 8.4 Hz, 2H), 7.70–7.63 (m, 4H), 7.44–7.42 (d, *J* = 8.8 Hz, 2H), 3.21 (s, 3H), 3.05–3.03 (m, 2H), 2.61–2.57 (m, 2H). LC/MS (ESI<sup>+</sup>): Calculated for C<sub>20</sub>H<sub>17</sub>ClF<sub>3</sub>N<sub>3</sub>O<sub>3</sub>S 471.06; Observed *m/z* [M+H]<sup>+</sup> 472.1, 474.1; HPLC purity: 98%.

**3-(3-(4-chlorophenyl)-1-(6-(trifluoromethyl)pyridin-3-yl)-1*H*-pyrazol-4-yl)-*N*-(methylsulfonyl)propanamide (10).**

**Method 1.:** Yield: 22%. <sup>1</sup>H NMR (400 MHz, Methanol-*d*<sub>4</sub>) δ 9.22 (d, *J* = 2.5 Hz, 1H), 8.42 (ddd, *J* = 8.6, 2.6, 0.8 Hz, 1H), 8.34 (d, *J* = 0.9 Hz, 1H), 7.92 (dd, *J* = 8.6, 0.7 Hz, 1H), 7.80 – 7.62 (m, 2H), 7.56 – 7.43 (m, 2H), 3.21 (s, 3H), 3.11 – 2.97 (m, 2H), 2.66 (t, *J* = 7.3 Hz, 2H). <sup>13</sup>C NMR (151 MHz, Methanol-*d*<sub>4</sub>) δ 174.2, 153.4, 145.6 (q, *J* = 35.4 Hz), 141.1, 139.7, 135.5, 132.8, 130.6 (2C), 129.9, 129.4, 127.7, 125.7, 123.9, 122.7 (d, *J* = 10.1 Hz), 122.1, 41.4, 37.3, 20.5. LC/MS (APCI<sup>+</sup>): Calculated for C<sub>19</sub>H<sub>16</sub>ClF<sub>3</sub>N<sub>4</sub>O<sub>3</sub>S 472.06; Observed *m/z* [M+H]<sup>+</sup> 473.0; HPLC purity: >99%.

**3-(3-(4-chlorophenyl)-1-(4-cyanophenyl)-1*H*-pyrazol-4-yl)-*N*-(methylsulfonyl)propanamide (11).**

**Method 3.:** Yield: 33%. <sup>1</sup>H NMR (400 MHz, Chloroform-*d*) δ 7.96 (s, 1H), 7.89–7.87 (m, 2H), 7.78–7.76 (m, 2H), 7.67–7.65 (m, 2H), 7.49–7.47 (m, 2H), 3.31 (s, 3H), 3.14–3.10 (m, 2H), 2.63–2.59 (m, 2H). LC/MS (APCI<sup>+</sup>): Calculated for C<sub>20</sub>H<sub>17</sub>ClN<sub>4</sub>O<sub>3</sub>S 428.07; Observed *m/z* [M+H]<sup>+</sup> 429.1; HPLC purity: >99%.

**3-(3-(4-chlorophenyl)-1-(4-(methylsulfinyl)phenyl)-1*H*-pyrazol-4-yl)-*N*-(methylsulfonyl)propanamide (12).**

**Step 1.:** 3-(3-(4-chlorophenyl)-1-(4-(methylthio)phenyl)-1*H*-pyrazol-4-yl)-*N*-(methylsulfonyl)propanamide from acid **631** following sulfonamide coupling method 2 (Scheme S1). Yield: 40 mg (31%). <sup>1</sup>H NMR (400 MHz, Chloroform-*d*) 7.83 (s, 1H), 7.67–7.65 (m, 4H), 7.47–7.46 (m, 3H), 7.45–7.34 (m, 2H), 3.28 (s, 3H), 3.12–3.08 (m, 2H), 2.62–2.58 (m, 2H), 2.54 (s, 3H). LC/MS (APCI<sup>+</sup>): Calculated for C<sub>20</sub>H<sub>20</sub>ClN<sub>3</sub>O<sub>3</sub>S<sub>2</sub> 449.06; Observed *m/z* [M+H]<sup>+</sup> 450.0; HPLC purity: 95%.

**Step 2.:** To a solution of 3-(3-(4-chlorophenyl)-1-(4-(methylthio)phenyl)-1*H*-pyrazol-4-yl)-*N*-(methylsulfonyl)propanamide (35 mg, 77.78 μmol) in MeOH (200 μL) and THF (200 μL) was added NaO<sub>4</sub> (17 mg, 81.67 μmol, 5 μL). The mixture was stirred at 20 °C for 15 h. The reaction mixture was diluted with aqueous Na<sub>2</sub>SO<sub>3</sub> (5 mL) and extracted with EtOAc (10 mL x 2). The combined organic layers were dried over Na<sub>2</sub>SO<sub>4</sub> and concentrated. The residue was purified by prep-HPLC (column: Phenomenex Synergi C18 150×25×10μm; mobile phase: [water (0.225% FA)-ACN]; B%: 35%-65%, 12min) to give 3-(3-(4-chlorophenyl)-1-(4-(methylsulfinyl)phenyl)-1*H*-pyrazol-4-yl)-*N*-(methylsulfonyl)propanamide (**12**). Yield: 21 mg (58%). <sup>1</sup>H NMR (400 MHz, Chloroform-*d*) δ 7.90–7.88 (m, 3H), 7.73–7.66 (m, 4H), 7.48–7.46 (m, 2H), 3.30 (s, 3H), 3.13–3.09 (m, 2H), 2.78 (s, 3H), 2.67–2.64 (m, 2H). LC/MS (APCI<sup>+</sup>): Calculated for C<sub>20</sub>H<sub>20</sub>ClN<sub>3</sub>O<sub>4</sub>S<sub>2</sub> 465.06; Observed *m/z* [M+H]<sup>+</sup> 466.0, 468.0; HPLC purity: >99%.

**3-(1-(4-bromophenyl)-3-phenyl-1*H*-pyrazol-4-yl)-*N*-(methylsulfonyl)propanamide (13).**

**Method 2.:** Yield: 29%. <sup>1</sup>H NMR (400 MHz, Chloroform-*d*) δ 7.76 (s, 1H), 7.62–7.60 (m, 2H), 7.57–7.38 (m, 7H), 3.18 (s, 3H), 3.06–3.02 (t, *J* = 7.2 Hz, 2H), 2.51–2.48 (t, *J* = 7.2 Hz, 2H). LC/MS (APCI<sup>+</sup>): Calculated for C<sub>19</sub>H<sub>18</sub>BrN<sub>3</sub>O<sub>3</sub>S 447.03; Observed *m/z* [M+H]<sup>+</sup> 448.0; HPLC purity: 99%.

**3-(1-(4-bromophenyl)-3-(3-chlorophenyl)-1*H*-pyrazol-4-yl)-*N*-(methylsulfonyl)propanamide (14).**

**Method 2.:** Yield: 10%. <sup>1</sup>H NMR (400 MHz, Chloroform-*d*) δ 7.83 (s, 1H), 7.70 (s, 1H), 7.64–7.53 (m, 5H), 7.43–7.34 (m, 2H), 3.26 (s, 3H), 3.07 (t, *J* = 7.2 Hz, 2H), 2.58 (t, *J* = 7.2 Hz, 2H). LC/MS (APCI<sup>+</sup>): Calculated for C<sub>19</sub>H<sub>17</sub>BrClN<sub>3</sub>O<sub>3</sub>S 480.99; Observed *m/z* [M+H]<sup>+</sup> 482.0, 484.0; HPLC purity: >99%.



**3-(3-(2-chlorophenyl)-1-(4-chlorophenyl)-1H-pyrazol-4-yl)-N-(methylsulfonyl)propanamide (15).**

**Method 1.:** Yield: 9%. <sup>1</sup>H NMR (300 MHz, Methanol-*d*<sub>4</sub>) δ 8.13 (d, *J* = 0.8 Hz, 1H), 7.73 (d, *J* = 8.9 Hz, 2H), 7.57 – 7.52 (m, 1H), 7.50 – 7.36 (m, 5H), 3.17 (s, 3H), 2.76 (t, *J* = 7.4 Hz, 2H), 2.58 – 2.43 (m, 2H). LC/MS (APCI<sup>+</sup>): Calculated for C<sub>19</sub>H<sub>17</sub>Cl<sub>2</sub>N<sub>3</sub>O<sub>3</sub>S 437.04; Observed *m/z* [M+H]<sup>+</sup> 437.9, 439.9 (chlorine isotopic pattern); HPLC purity: >99%.

**3-(1-(4-bromophenyl)-3-(pyridin-4-yl)-1H-pyrazol-4-yl)-N-(methylsulfonyl)propanamide (16).**

**Method 3.:** Yield: 19%. <sup>1</sup>H NMR (400MHz, DMSO-*d*<sub>6</sub>) δ 8.74–8.63 (m, 2H), 8.51–8.47 (m, 1H), 7.88–7.83 (m, 2H), 7.74 (s, 4H), 3.10–3.07 (s, 3H), 2.99–2.93 (m, 2H), 2.59–2.55 (m, 2H). <sup>13</sup>C NMR (151 MHz, DMSO-*d*<sub>6</sub>) δ 172.3, 150.1 (2C), 147.9, 140.2, 138.5, 132.4 (2C), 128.4, 121.6 (2C), 121.2, 120.2 (2C), 118.8, 40.9, 36.1, 19.4. LC/MS (APCI<sup>+</sup>): Calculated for C<sub>18</sub>H<sub>17</sub>BrN<sub>4</sub>O<sub>3</sub>S 448.02; Observed *m/z* [M+H]<sup>+</sup> 449.0; HPLC purity: 97%.

**3-(1-(4-bromophenyl)-3-(pyridin-3-yl)-1H-pyrazol-4-yl)-N-(methylsulfonyl)propanamide (17).**

**Method 3.:** Yield: 6%. <sup>1</sup>H NMR (400 MHz, Chloroform-*d*) δ 8.79 (s, 1H), 8.45–8.44 (d, *J* = 4.4 Hz, 1H), 8.04–8.02 (d, *J* = 7.6 Hz, 1H), 7.83 (s, 1H), 7.56–7.50 (m, 4H), 7.31–7.30 (m, 1H), 3.19 (s, 3H), 3.01 (m, 2 H), 2.59–2.56 (m, 2H). <sup>13</sup>C NMR (151 MHz, Chloroform-*d*) δ 171.8, 147.7, 147.1, 146.6, 138.7, 137.0, 132.7, 132.6, 130.4, 128.1, 127.0, 124.6, 120.5, 120.2, 119.9, 41.7, 37.3, 19.8. LC/MS (APCI<sup>+</sup>): Calculated for C<sub>18</sub>H<sub>17</sub>BrN<sub>4</sub>O<sub>3</sub>S 448.02; Observed *m/z* [M+H]<sup>+</sup> 449.0, 451.0 (1:1) bromine isotopic pattern; HPLC purity: >99%.

**3-(1-(4-bromophenyl)-3-(pyrazin-2-yl)-1H-pyrazol-4-yl)-N-(methylsulfonyl)propanamide (18).**

**Method 2.:** Yield: 12%. <sup>1</sup>H NMR (400 MHz, Chloroform-*d*) δ 9.44 (s, 1H), 8.67 (brs, 1H), 8.58 (s, 1H), 7.91 (s, 1H), 7.63 (q, *J* = 9.0 Hz, 4H), 3.28–3.19 (m, 5H), 2.79 (t, *J* = 7.1 Hz, 2H). LC/MS (APCI<sup>+</sup>): Calculated for C<sub>17</sub>H<sub>16</sub>BrN<sub>5</sub>O<sub>3</sub>S 449.02; Observed *m/z* [M+H]<sup>+</sup> 449.8, 451.9 (1:1) bromine isotopic pattern; HPLC purity: 91%.

**3-(1-(4-bromophenyl)-3-cyclohexyl-1H-pyrazol-4-yl)-N-(methylsulfonyl)propanamide (19).**

**Method 2.:** Yield: 40%. <sup>1</sup>H NMR (400 MHz, Chloroform-*d*) δ 8.17 (s, 1H), 7.65 (s, 1H), 7.52 (s, 4H), 3.30 (s, 3H), 2.93–2.82 (m, 2H), 2.60 (s, 3H), 1.88 (brs, 4H), 1.80–1.62 (m, 3H), 1.35 (s, 3H). LC/MS (APCI<sup>+</sup>): Calculated for C<sub>19</sub>H<sub>24</sub>BrN<sub>3</sub>O<sub>3</sub>S 453.07; Observed *m/z* [M+H]<sup>+</sup> 454.0; HPLC purity: >99%.

**3-(1-(4-bromophenyl)-3-(tetrahydro-2H-pyran-4-yl)-1H-pyrazol-4-yl)-N-(methylsulfonyl)propanamide (20).**

**Method 2.:** Yield: 13%. <sup>1</sup>H NMR (400MHz, DMSO-*d*<sub>6</sub>) δ 8.18 (s, 1H), 7.71–7.62 (m, 4H), 3.94–3.92 (m, 2H), 3.46–3.45 (m, 2H), 3.43–3.26 (m, 2H), 3.07 (s, 3H), 2.70–2.69 (m, 1H), 2.67–2.66 (m, 3H), 1.77–1.73 (m, 4H). <sup>13</sup>C NMR (151 MHz, DMSO-*d*<sub>6</sub>) δ 172.7, 155.6, 138.9, 132.2 (2C), 126.2, 119.7, 119.4 (2C), 117.4, 67.1 (2C), 40.9, 36.9, 32.6, 31.9

(2C), 18.4. LC/MS (APCI<sup>+</sup>): Calculated for C<sub>18</sub>H<sub>22</sub>BrN<sub>3</sub>O<sub>4</sub>S 455.05; Observed *m/z* [M+H]<sup>+</sup> + 456.0; HPLC purity: 98%.

**3-(1-(4-bromophenyl)-3-(piperidin-4-yl)-1*H*-pyrazol-4-yl)-*N*-(methylsulfonyl)propanamide (21).**

**Step 1.:** *Tert*-butyl 4-(1-(4-bromophenyl)-4-(3-(methylsulfonamido)-3-oxopropyl)-1*H*-pyrazol-3-yl)piperidine-1-carboxylate was obtained as a white solid. Yield: 60 mg (17%) from acid **67h** by sulfonamide coupling method 2 (Scheme S2). LC/MS (APCI<sup>+</sup>): Calculated for C<sub>23</sub>H<sub>31</sub>BrN<sub>4</sub>O<sub>5</sub>S 554.12; Observed *m/z* [M+H-Boc]<sup>+</sup> 455.0; HPLC purity: 83%.

**Step 2.:** The mixture of *tert*-butyl 4-(1-(4-bromophenyl)-4-(3-(methylsulfonamido)-3-oxopropyl)-1*H*-pyrazol-3-yl)piperidine-1-carboxylate (55 mg, 99.01 μmol) in TFA (100 μL) and DCM (1 mL) was stirred at 20 °C for 2 h. The reaction mixture was concentrated. The obtained residue was purified by prep-HPLC (column: Phenomenex Synergi C18 150×25×10um; mobile phase: [water (0.225%FA)-ACN]; B%: 5%-35%, 12min) to give 3-(1-(4-bromophenyl)-3-(piperidin-4-yl)-1*H*-pyrazol-4-yl)-*N*-(methylsulfonyl)propanamide (**21**) as a white solid. Yield: 27 mg (59%). <sup>1</sup>H NMR (400MHz, DMSO-*d*<sub>6</sub>) δ 8.22 (s, 1H), 7.71–7.62 (m, 4H), 3.36–3.33 (m, 3H), 3.06 (s, 3H), 2.77–2.63 (m, 2H), 2.49–2.27 (m, 2H), 2.01–1.91 (m, 4H). LC/MS (APCI<sup>+</sup>): Calculated for C<sub>18</sub>H<sub>23</sub>BrN<sub>4</sub>O<sub>3</sub>S 454.07; Observed *m/z* [M+H]<sup>+</sup> 455.0; HPLC purity: 99%.

**3-(1-(4-bromophenyl)-3-(1-formylpiperidin-4-yl)-1*H*-pyrazol-4-yl)-*N*-(methylsulfonyl)propanamide (22).**

**Method 2.:** Yield: 32%. <sup>1</sup>H NMR (400MHz, DMSO-*d*<sub>6</sub>) δ 8.21 (s, 1H), 8.03 (s, 1H), 7.71–7.63 (m, 4H), 4.26–4.22 (m, 1H), 3.79–3.76 (m, 1H), 3.19 (s, 3H), 3.00–2.80 (m, 1H), 2.79–2.59 (m, 6H), 2.34–1.54 (m, 4H). LC/MS (APCI<sup>+</sup>): Calculated for C<sub>19</sub>H<sub>23</sub>BrN<sub>4</sub>O<sub>4</sub>S 482.06; Observed *m/z* [M+H]<sup>+</sup> 483.1; HPLC purity: >99%.

**3-(1-(4-bromophenyl)-3-(4-nitrophenyl)-1*H*-pyrazol-4-yl)-*N*-(methylsulfonyl)propanamide (23).**

**Method 2.:** Yield: 71%. <sup>1</sup>H NMR (400 MHz, Methanol-*d*<sub>4</sub>) δ 8.38 – 8.30 (m, 2H), 8.22 (d, *J* = 6.3 Hz, 1H), 8.06 – 7.98 (m, 2H), 7.82 – 7.74 (m, 2H), 7.69 – 7.61 (m, 2H), 3.16 (s, 3H), 3.09 (t, *J* = 7.5 Hz, 2H), 2.65 (t, *J* = 7.5 Hz, 2H). LC/MS (ESI<sup>+</sup>): Calculated for C<sub>19</sub>H<sub>17</sub>BrN<sub>4</sub>O<sub>5</sub>S 492.01; Observed *m/z* [M+H]<sup>+</sup> 493.0, 495.0 (1:1) bromine isotopic pattern; HPLC purity: 93%.

**3-(3-(4-aminophenyl)-1-(4-bromophenyl)-1*H*-pyrazol-4-yl)-*N*-(methylsulfonyl)propanamide (24).**—

To a mixture of 3-(1-(4-bromophenyl)-3-(4-nitrophenyl)-1*H*-pyrazol-4-yl)-*N*-(methylsulfonyl)propanamide (**23**) (100 mg, 0.203 mmol) and iron (53 mg, 0.953 mmol) in EtOH (2 mL) was added saturated solution of NH<sub>4</sub>Cl (1 mL) and heated to 80 °C for 18 h. The reaction mixture was cooled to 25 °C and separated the organic layer. The organic layer was dried over Na<sub>2</sub>SO<sub>4</sub> and evaporated the solvent under reduced pressure. The residue was purified by flash silica gel column using DCM: MeOH (0–5% gradient) as eluents to afford 3-(3-(4-aminophenyl)-1-(4-bromophenyl)-1*H*-pyrazol-4-yl)-*N*-(methylsulfonyl)propanamide (**24**) as a grey solid. Yield: 5 mg

(5%).  $^1\text{H}$  NMR (400 MHz, Methanol- $d_4$ )  $\delta$  8.19 (s, 1H), 7.90 (d,  $J$  = 8.5 Hz, 2H), 7.76 (d,  $J$  = 8.8 Hz, 2H), 7.66 (d,  $J$  = 8.8 Hz, 2H), 7.49 (d,  $J$  = 8.5 Hz, 2H), 3.23 (s, 3H), 3.06 (t,  $J$  = 7.4 Hz, 2H), 2.68 (t,  $J$  = 7.4 Hz, 2H). LC/MS (APCI $^+$ ): Calculated for  $\text{C}_{19}\text{H}_{19}\text{BrN}_4\text{O}_3\text{S}$  462.04; Observed  $m/z$   $[\text{M}+\text{H}]^+$  463.1, 465.1 (1:1) bromine isotopic pattern; HPLC purity: 92%.

**3-(3-benzyl-1-(4-bromophenyl)-1H-pyrazol-4-yl)-N-(methylsulfonyl)propanamide (25).**

**Method 3.:** Yield: 20%.  $^1\text{H}$  NMR (400 MHz, Chloroform- $d$ )  $\delta$  7.71 (s, 1H), 7.58 (s, 4H), 7.36–7.32 (m, 5H), 4.09 (s, 2H), 3.21 (s, 3H), 2.74–2.71 (m, 2H), 2.06–2.02 (m, 2H). LC/MS (APCI $^+$ ): Calculated for  $\text{C}_{20}\text{H}_{20}\text{BrN}_3\text{O}_3\text{S}$  461.04; Observed  $m/z$   $[\text{M}+\text{H}]^+$  462.0; HPLC purity: >99%.

**3-(1-(4-bromophenyl)-3-(4-chlorophenyl)-1H-pyrazol-4-yl)propanoic acid (26).**

—To a solution of (*E*)-3-(1-(4-bromophenyl)-3-(4-chlorophenyl)-1H-pyrazol-4-yl)acrylic acid (**62a**) (1.66 g, 4.11 mmol) in MeOH (150 mL) was added  $\text{NH}_2\text{NH}_2 \cdot \text{H}_2\text{O}$  (16.47 g, 328.99 mmol, 16 mL) and the mixture was heated to 80 °C for 48 h (Scheme S1). The mixture was cooled to room temperature, diluted with ice-water (100 mL) and adjusted pH = 3 with 1 M HCl. The aqueous layer was extracted with DCM (50 mL x 3). The organic layer was washed with brine (50 mL), dried over anhydrous  $\text{Na}_2\text{SO}_4$  and concentrated. To the residue was added petroleum ether (20 mL) slowly. The mixture was concentrated slowly to give some solid. The solid collected to give 3-(1-(4-bromophenyl)-3-(4-chlorophenyl)-1H-pyrazol-4-yl)propanoic acid (**26**) as a yellow solid. Yield: 1.80 g (99%).  $^1\text{H}$  NMR (400 MHz, Chloroform- $d$ )  $\delta$  7.85–7.75 (m, 1H), 7.59 (d,  $J$  = 7.8 Hz, 6H), 7.48–7.38 (m, 2H), 3.02 (m, 2H), 2.67 (m, 2H). LC/MS (APCI $^+$ ): Calculated for  $\text{C}_{18}\text{H}_{14}\text{BrClN}_2\text{O}$  403.99; Observed  $m/z$   $[\text{M}+\text{H}]^+$  404.9, 407.0; HPLC purity: 92%.

**3-(1-(4-bromophenyl)-3-(4-chlorophenyl)-1H-pyrazol-4-yl)-N-methylpropanamide (27).**

**Method 3.:** To a solution of  $\text{MeNH}_2/\text{THF}$  (2 M, 5 mL) was added the solution of 3-(1-(4-bromophenyl)-3-(4-chlorophenyl)-1H-pyrazol-4-yl)propanoyl chloride (**68**) (220 mg, 518.72  $\mu\text{mol}$ ) in DCM (2 mL) at –50 °C (Scheme S3). The mixture was stirred at –30 °C for ~3 h. The mixture was washed with water (5 mL) and concentrated. The residue was purified by prep-HPLC to give 3-(1-(4-bromophenyl)-3-(4-chlorophenyl)-1H-pyrazol-4-yl)-N-methylpropanamide (**27**) as a light-yellow solid. Yield: 60 mg (27%).  $^1\text{H}$  NMR (300 MHz, DMSO- $d_6$ )  $\delta$  8.42 (s, 1H), 7.85–7.81 (m, 2H), 7.77–7.75 (m, 2H), 7.72–7.70 (m, 2H), 7.56–7.54 (m, 2H), 2.89 (t,  $J$  = 7.6 Hz, 2H), 2.56 (d,  $J$  = 8.4 Hz, 3H), 2.43 (t,  $J$  = 7.6 Hz, 2H). LC/MS (APCI $^+$ ): Calculated for  $\text{C}_{19}\text{H}_{17}\text{BrClN}_3\text{O}$  417.02; Observed  $m/z$   $[\text{M}+\text{H}]^+$  418.0, 420.0; HPLC purity: 98%.

**3-(1-(4-bromophenyl)-3-(4-chlorophenyl)-1H-pyrazol-4-yl)-N-methyl-N-(methylsulfonyl)propanamide (28).**—To a solution of *N*-methylmethanesulfonamide (116 mg, 1.06 mmol) in THF (5.00 mL) was added NaH 60% dispersion (45 mg, 1.13 mmol) at 0–10 °C. After stirred at 15 °C for 1 h, a solution of 3-(1-(4-bromophenyl)-3-(4-chlorophenyl)-1H-pyrazol-4-yl)propanoyl chloride (**68**) (300 mg, 707.35  $\mu\text{mol}$ ) in DCM (3.00 mL) was added at –10 °C *via* syringe. The mixture was stirred

at 15 °C for another 2 h. The mixture was washed with brine (5 mL) and concentrated. The residue was purified by prep-HPLC to give 3-(1-(4-bromophenyl)-3-(4-chlorophenyl)-1*H*-pyrazol-4-yl)-*N*-methyl-*N*-(methylsulfonyl)propanamide (**28**). Yield: 65 mg (17%).

<sup>1</sup>H NMR (300 MHz, Methanol-*d*<sub>4</sub>) δ 8.25–8.17 (m, 1H), 7.80–7.71 (m, 4H), 7.69–7.61 (m, 2H), 7.54–7.46 (m, 2H), 3.27 (s, 6H), 3.11–2.98 (m, 4H). LC/MS (APCI<sup>+</sup>): Calculated for C<sub>20</sub>H<sub>19</sub>BrClN<sub>3</sub>O<sub>3</sub>S 495.00; Observed *m/z* [M+H]<sup>+</sup> 496.0, 498.0; HPLC purity: 98%.

***N*-(3-(1-(4-bromophenyl)-3-(4-chlorophenyl)-1*H*-pyrazol-4-yl)propyl)methanesulfonamide (29).**—

To a solution of 3-(1-(4-bromophenyl)-3-(4-chlorophenyl)-1*H*-pyrazol-4-yl)propan-1-amine (**72**) (90 mg, 230.36 μmol) in DCM (3 mL) were added Et<sub>3</sub>N (93 mg, 921.44 μmol, 128 μL) and MsCl (36 μL) at 0–10 °C (Scheme S3). The mixture was stirred at 10 °C for 1 h. The mixture was quenched with water (2 mL) and extracted with DCM (5 mL x 2). The organic phase was concentrated and purified by reverse phase HPLC to give *N*-(3-(1-(4-bromophenyl)-3-(4-chlorophenyl)-1*H*-pyrazol-4-yl)propyl)methanesulfonamide (**29**) as a white solid. Yield: 68 mg (63%). <sup>1</sup>H NMR (400MHz, DMSO-*d*<sub>6</sub>) δ 8.54 – 8.41 (m, 1H), 7.91 – 7.81 (m, 2H), 7.81 – 7.74 (m, 2H), 7.74 – 7.66 (m, 2H), 7.60 – 7.48 (m, 2H), 7.12 – 7.00 (m, 1H), 3.10 – 2.96 (m, 2H), 2.89 (s, 3H), 2.76 – 2.69 (m, 2H), 1.87 – 1.73 (m, 2H). LC/MS (APCI<sup>+</sup>): Calculated for C<sub>19</sub>H<sub>19</sub>BrClN<sub>3</sub>O<sub>2</sub>S 467.01; Observed *m/z* [M+H]<sup>+</sup> 468.0; HPLC purity: >99%.

***N*-((2-(1-(4-bromophenyl)-3-(4-chlorophenyl)-1*H*-pyrazol-4-yl)ethyl)sulfonyl)acetamide (30).**—

To the solution of 2-(1-(4-bromophenyl)-3-(4-chlorophenyl)-1*H*-pyrazol-4-yl)ethane-1-sulfonamide (**74**) (150 mg, 340.34 μmol) and Et<sub>3</sub>N (69 mg, 680.68 μmol, 94 μL) in THF (4 mL) was added acetyl chloride (40 mg, 510.51 μmol, 36 μL) drop-wise in ice-bath (Scheme S4). The mixture was stirred at 40 °C for 16 h. The mixture was concentrated and separated between water (3 mL) and EtOAc (3 mL). The organic phase was dried over anhydrous Na<sub>2</sub>SO<sub>4</sub> and concentrated. The residue was purified by prep-HPLC (column: Phenomenex Synergi C18150×25×10um; mobile phase: [water (0.225%FA)-ACN]; B%: 57%-87%, 10min) and then purified again by prep-HPLC (column: Phenomenex Gemini 150×25mmx10um; mobile phase: [water (0.05% ammonia hydroxide v/v)-ACN]; B%: 22%-52%, 10min) to afford *N*-((2-(1-(4-bromophenyl)-3-(4-chlorophenyl)-1*H*-pyrazol-4-yl)ethyl)sulfonyl)acetamide (**30**) as a white solid. Yield: 29 mg (17%). <sup>1</sup>H NMR (400 MHz, DMSO-*d*<sub>6</sub>) δ 8.58 (s, 1H), 7.88–7.83 (m, 3H), 7.74–7.70 (m, 4H), 7.54–7.51 (m, 2H), 3.60–3.56 (m, 2H), 3.06–3.03 (m, 2H), 1.87 (s,3H). LC/MS (APCI<sup>+</sup>): Calculated for C<sub>19</sub>H<sub>17</sub>BrClN<sub>3</sub>O<sub>3</sub>S 480.99; Observed *m/z* [M+H]<sup>+</sup> 482.0; HPLC purity: >99%.

**2-(1-(4-bromophenyl)-3-(4-chlorophenyl)-1*H*-pyrazol-4-yl)-*N*-(methylsulfonyl)acetamide (31).**

**Method 2.:** Yield: 11%. <sup>1</sup>H NMR (400 MHz, Chloroform-*d*) δ 8.05 (s, 1H), 7.88 (s, 1H), 7.67–7.60 (m, 6H), 7.49–7.47 (d, *J* = 8.4 Hz, 2H), 3.81 (s, 2H), 3.15 (s, 3H). LC/MS (APCI<sup>+</sup>): Calculated for C<sub>18</sub>H<sub>15</sub>BrClN<sub>3</sub>O<sub>3</sub>S 466.97; Observed *m/z* [M+H]<sup>+</sup> 467.9, 470.0; HPLC purity: 99%.

**4-(1-(4-bromophenyl)-3-(4-chlorophenyl)-1H-pyrazol-4-yl)-N-(methylsulfonyl)butanamide (32).**

**Method 2.:** Yield: 9%. <sup>1</sup>H NMR (300 MHz, Methanol-*d*<sub>4</sub>) δ 8.20 (s, 1H), 7.78–7.72 (m, 4H), 7.66–7.64 (m, 2H), 7.50–7.48 (m, 2H), 3.17 (s, 3H), 2.79–2.75 (t, *J* = 7.6 Hz, 2H), 2.39–2.36 (t, *J* = 7.2 Hz, 2H), 1.99–1.95 (t, *J* = 7.6 Hz, 2H). LC/MS (APCI<sup>+</sup>): Calculated for C<sub>20</sub>H<sub>19</sub>BrClN<sub>3</sub>O<sub>3</sub>S 495.00; Observed *m/z* [M+H]<sup>+</sup> 496.0; HPLC purity: 96%.

**3-(1-(4-bromophenyl)-3-(4-chlorophenyl)-1H-pyrazol-4-yl)-N(ethylsulfonyl)propanamide (33).**

**Method 1.:** Yield: 23%. <sup>1</sup>H NMR (300 MHz, Methanol-*d*<sub>4</sub>) δ 8.14 (s, 1H), 7.73 (ddt, *J* = 7.5, 4.7, 2.4 Hz, 4H), 7.69 – 7.61 (m, 2H), 7.53 – 7.46 (m, 2H), 3.42 – 3.35 (m, 2H), 3.05 (t, *J* = 7.3 Hz, 2H), 2.66 (t, *J* = 7.3 Hz, 2H), 1.25 (t, *J* = 7.4 Hz, 3H). LC/MS (ESI<sup>+</sup>): Calculated for C<sub>20</sub>H<sub>19</sub>BrClN<sub>3</sub>O<sub>3</sub>S 495.00; Observed *m/z* [M+H]<sup>+</sup> 496.1; HPLC purity: 98%.

**3-(1-(4-bromophenyl)-3-(4-chlorophenyl)-1H-pyrazol-4-yl)-N-(cyclopropylsulfonyl)propanamide (34).**

**Method 1.:** Yield: 25 mg (10%). <sup>1</sup>H NMR (300 MHz, Methanol-*d*<sub>4</sub>) δ 8.15 (s, 1H), 7.80 – 7.67 (m, 4H), 7.68 – 7.62 (m, 2H), 7.54 – 7.46 (m, 2H), 3.05 (t, *J* = 7.3 Hz, 2H), 2.98 – 2.86 (m, 1H), 2.65 (t, *J* = 7.3 Hz, 2H), 1.26 – 1.13 (m, 2H), 1.08 – 0.98 (m, 2H). LC/MS (APCI<sup>+</sup>): Calculated for C<sub>21</sub>H<sub>19</sub>BrClN<sub>3</sub>O<sub>3</sub>S 507.00; Observed *m/z* [M+H]<sup>+</sup> 508.1; HPLC purity: >99%.

**3-(1-(4-chlorophenyl)-3-(pyridin-4-yl)-1H-pyrazol-4-yl)-N-(methylsulfonyl)propanamide (35).**

**Method 1.:** Yield: 8%. <sup>1</sup>H NMR (300 MHz, Methanol-*d*<sub>4</sub>) δ 8.68 – 8.58 (m, 2H), 8.21 (s, 1H), 7.89 – 7.80 (m, 4H), 7.57 – 7.48 (m, 2H), 3.23 (s, 3H), 3.14 (t, *J* = 7.4 Hz, 2H), 2.71 (t, *J* = 7.3 Hz, 2H). LC/MS (ESI<sup>+</sup>): Calculated for C<sub>18</sub>H<sub>17</sub>ClN<sub>4</sub>O<sub>3</sub>S 404.07; Observed *m/z* [M+H]<sup>+</sup> 405.1; HPLC purity: >99%.

**3-(1-(4-chlorophenyl)-3-(pyridin-4-yl)-1H-pyrazol-4-yl)-2-methyl-N-(methylsulfonyl)propanamide (36).**

**Method 1.:** Yield: 18%. <sup>1</sup>H NMR (300 MHz, Methanol-*d*<sub>4</sub>) δ 8.68 – 8.61 (m, 2H), 8.17 (s, 1H), 7.88 – 7.80 (m, 4H), 7.56 – 7.49 (m, 2H), 3.15 (s, 4H), 2.98 – 2.84 (m, 1H), 2.80 – 2.66 (m, 1H), 1.25 (d, *J* = 6.9 Hz, 3H). LC/MS (ESI<sup>+</sup>): Calculated for C<sub>19</sub>H<sub>19</sub>ClN<sub>4</sub>O<sub>3</sub>S 418.09; Observed *m/z* [M+H]<sup>+</sup> 419.1; HPLC purity: >99%.

**3-(1-(4-chlorophenyl)-3-(pyridin-4-yl)-1H-pyrazol-4-yl)-N-(methylsulfonyl)butanamide (37).**

**Method 1.:** Yield: 21%. <sup>1</sup>H NMR (300 MHz, Methanol-*d*<sub>4</sub>) δ 8.62 (d, *J* = 5.0 Hz, 2H), 8.28 (s, 1H), 7.94 – 7.76 (m, 4H), 7.51 (d, *J* = 8.9 Hz, 2H), 3.64 (q, *J* = 7.2 Hz, 1H), 3.10 (s, 3H), 2.75 – 2.54 (m, 2H), 1.35 (d, *J* = 7.2 Hz, 3H). LC/MS (ESI<sup>+</sup>): Calculated for C<sub>19</sub>H<sub>19</sub>ClN<sub>4</sub>O<sub>3</sub>S 418.09; Observed *m/z* [M+H]<sup>+</sup> 419.1; HPLC purity: >99%.

**(E)-3-(1-(4-chlorophenyl)-3-(pyridin-4-yl)-1H-pyrazol-4-yl)-N-(methylsulfonyl)acrylamide (38).**

**Method 1.:** Isolated as hydrochloride salt. Yield: 21%. <sup>1</sup>H NMR (300 MHz, DMSO-*d*<sub>6</sub>) δ 9.24 (s, 1H), 8.94 (d, *J* = 5.6 Hz, 2H), 8.10 (d, *J* = 5.7 Hz, 2H), 8.04 – 8.00 (m, 2H), 7.76 – 7.65 (m, 3H), 6.57 (d, *J* = 15.8 Hz, 1H), 3.32 (s, 3H). <sup>13</sup>C NMR (101 MHz, DMSO-*d*<sub>6</sub>) δ 164.4, 147.5, 145.5, 144.3 (2C), 137.4, 132.5, 132.1, 130.5, 129.7 (2C), 124.6 (2C), 120.9 (2C), 119.1, 118.6, 41.3. LC/MS (ESI<sup>+</sup>): Calculated for C<sub>18</sub>H<sub>15</sub>ClN<sub>4</sub>O<sub>3</sub>S 402.06; Observed *m/z* [M+H]<sup>+</sup> 403.0, 404.9; HPLC purity: 98%.

**(E)-3-(1-(4-bromophenyl)-3-(pyridin-4-yl)-1H-pyrazol-4-yl)-N-(methylsulfonyl)acrylamide (39).**

**Method 1.:** Yield: 10%. <sup>1</sup>H NMR (300 MHz, Methanol-*d*<sub>4</sub>) δ 9.02 – 8.90 (m, 3H), 8.49 – 8.43 (m, 2H), 7.97 – 7.87 (m, 3H), 7.81 – 7.71 (m, 2H), 6.61 (d, *J* = 15.5 Hz, 1H), 3.34 (s, 3H). LC/MS (ESI<sup>+</sup>): Calculated for C<sub>18</sub>H<sub>17</sub>BrN<sub>4</sub>O<sub>3</sub>S 448.02; Observed *m/z* [M+H]<sup>+</sup> 448.8; HPLC purity: 99%.

**2-(1-(4-chlorophenyl)-3-(pyridin-4-yl)-1H-pyrazol-4-yl)-N-(methylsulfonyl)cyclopropane-1-carboxamide (40).**

**Method 1.:** Yield: 39%. <sup>1</sup>H NMR (300 MHz, Methanol-*d*<sub>4</sub>) δ 8.91 – 8.83 (m, 2H), 8.60 – 8.52 (m, 2H), 8.41 (s, 1H), 7.96 – 7.89 (m, 2H), 7.62 – 7.55 (m, 2H), 3.35 (s, 3H), 2.78 – 2.68 (m, 1H), 1.96 (dt, *J* = 8.8, 4.7 Hz, 1H), 1.80 (dt, *J* = 9.3, 4.7 Hz, 1H), 1.58 (ddd, *J* = 8.1, 6.5, 4.3 Hz, 1H). <sup>13</sup>C NMR (151 MHz, Methanol-*d*<sub>4</sub>) δ 172.1, 161.4, 161.1, 147.5, 147.1, 146.5, 144.1, 143.8, 138.5, 132.4, 128.7, 123.7, 123.3, 122.9, 120.4, 40.2, 24.3, 17.5, 15.6. LC/MS (ESI<sup>+</sup>): C<sub>19</sub>H<sub>17</sub>ClN<sub>4</sub>O<sub>3</sub>S 416.07; Observed *m/z* [M+H]<sup>+</sup> 417.1; HPLC purity: >99%.

**2-(1-(4-bromophenyl)-3-(pyridin-4-yl)-1H-pyrazol-4-yl)-N-(methylsulfonyl)cyclopropane-1-carboxamide (41).**

**Method 1.:** Yield: 22%. <sup>1</sup>H NMR (600 MHz, Methanol-*d*<sub>4</sub>) δ 8.74 (d, *J* = 5.7 Hz, 2H), 8.33 – 8.26 (m, 3H), 7.83 – 7.75 (m, 2H), 7.70 – 7.62 (m, 2H), 3.29 (s, 4H), 2.63 (ddd, *J* = 8.9, 6.6, 4.7 Hz, 1H), 1.88 (dt, *J* = 8.2, 4.7 Hz, 1H), 1.73 (dt, *J* = 9.2, 4.7 Hz, 1H), 1.51 (ddd, *J* = 8.2, 6.6, 4.7 Hz, 1H). <sup>13</sup>C NMR (151 MHz, Methanol-*d*<sub>4</sub>) δ 173.6, 163.1, 162.9, 162.6, 148.5, 148.1, 148.0, 145.9, 145.6, 139.9, 130.1, 125.0, 124.6, 121.8, 121.7, 41.6, 25.8, 19.0, 17.0. LC/MS (ESI<sup>+</sup>): calculated for C<sub>19</sub>H<sub>17</sub>BrN<sub>4</sub>O<sub>3</sub>S 460.02; Observed *m/z* [M+H]<sup>+</sup> 460.9; HPLC purity: >98%.

**3-(3-(4-bromophenyl)-1-(4-chlorophenyl)-1H-pyrazol-5-yl)-N-(methylsulfonyl)propanamide (51).**

**Method 2.:** Yield: 25%. <sup>1</sup>H NMR (400 MHz, Chloroform-*d*) δ 8.00 (s, 1H), 7.72–7.70 (m, 2H), 7.56–7.45 (m, 6H), 6.53 (s, 1H), 3.30 (s, 3H), 3.11–3.07 (t, *J* = 7.2 Hz, 2H), 2.69–2.65 (t, *J* = 7.2 Hz, 2H). LC/MS (APCI<sup>+</sup>): Calculated for C<sub>19</sub>H<sub>17</sub>BrClN<sub>3</sub>O<sub>3</sub>S 480.99; Observed *m/z* [M+H]<sup>+</sup> 482.0; HPLC purity: 99%.

**3-(3-(4-chlorophenyl)-1-(4-fluorophenyl)-1H-pyrazol-5-yl)-N-(methylsulfonyl)propanamide (52).**

**Method 2.:** Yield: 20%. <sup>1</sup>H NMR (300 MHz, Methanol-*d*<sub>4</sub>) δ 7.85 – 7.76 (m, 2H), 7.64 – 7.53 (m, 2H), 7.46 – 7.39 (m, 2H), 7.39 – 7.28 (m, 2H), 6.71 (s, 1H), 3.21 (s, 3H), 3.00 (t, *J* = 7.3 Hz, 2H), 2.71 (t, *J* = 7.3 Hz, 2H). LC/MS (ESI<sup>+</sup>): Calculated for C<sub>19</sub>H<sub>17</sub>ClFN<sub>3</sub>O<sub>3</sub>S<sub>3</sub> 421.07; Observed *m/z* [M+H]<sup>+</sup> 422.1; HPLC purity: 96%.

**3-(1-(4-bromophenyl)-4-(4-chlorophenyl)-1H-pyrazol-3-yl)-N-(methylsulfonyl)propanamide (53).**

**Method 2.:** Yield: 15%. <sup>1</sup>H NMR (400 MHz, Chloroform-*d*) δ 10.70 (s, 1H), 8.00 (s, 1H), 7.64–7.45 (m, 4H), 7.43–7.41 (m, 2H), 7.34–7.32 (m, 2H), 3.32 (s, 3H), 3.19–3.16 (t, *J* = 6.4 Hz, 2H), 2.89–2.86 (t, *J* = 6.4 Hz, 2H). LC/MS (APCI<sup>+</sup>): Calculated for C<sub>19</sub>H<sub>17</sub>BrClN<sub>3</sub>O<sub>3</sub>S 480.99; Observed *m/z* [M+H]<sup>+</sup> 482.0; HPLC purity: 95%.

**3-(3,5-bis(4-chlorophenyl)-1H-pyrazol-1-yl)-N-(methylsulfonyl)propanamide (54).**

**Method 1.:** Yield: 11%. <sup>1</sup>H NMR (300 MHz, Methanol-*d*<sub>4</sub>) δ 7.89 – 7.79 (m, 2H), 7.60 – 7.49 (m, 4H), 7.45 – 7.36 (m, 2H), 6.73 (s, 1H), 4.45 (t, *J* = 6.5 Hz, 2H), 3.14 (s, 3H), 2.97 (t, *J* = 6.5 Hz, 2H). LC/MS (ESI<sup>+</sup>): Calculated for C<sub>19</sub>H<sub>17</sub>Cl<sub>2</sub>N<sub>3</sub>O<sub>3</sub>S 437.04; Observed *m/z* [M+H]<sup>+</sup> 438.0; HPLC purity: >99%.

**3-(5-(4-bromophenyl)-1-(4-chlorophenyl)-1H-pyrazol-3-yl)-N-(methylsulfonyl)propanamide (55).**

**Method 2.:** Yield: 34%. <sup>1</sup>H NMR (400 MHz, Chloroform-*d*) δ 10.71 (s, 1H), 7.50–7.49 (m, 2H), 7.38–7.36 (m, 2H), 7.27–7.25 (m, 2H), 7.11–7.09 (m, 2H), 6.37 (s, 1H), 3.30 (s, 3H), 3.13–3.11 (t, *J* = 6.0 Hz, 2H), 2.88–2.84 (t, *J* = 6.0 Hz, 2H). LC/MS (APCI<sup>+</sup>): Calculated for C<sub>19</sub>H<sub>17</sub>BrClN<sub>3</sub>O<sub>3</sub>S 480.99; Observed *m/z* [M+H]<sup>+</sup> 482.0; HPLC purity: >99%.

**3-(2,4-bis(4-chlorophenyl)oxazol-5-yl)-N-(methylsulfonyl)propanamide (56).**

**Method 3.:** Yield: 11%. <sup>1</sup>H NMR (400 MHz, Methanol-*d*<sub>4</sub>) δ 8.06 (d, *J* = 6.80 Hz, 2H), 7.76 (d, *J* = 6.80 Hz, 2H), 7.54 (d, *J* = 6.80 Hz, 2H), 7.49 (d, *J* = 6.80 Hz, 2H), 3.32 (t, *J* = 5.60 Hz, 2H), 3.22 (s, 3H), 2.85 (t, *J* = 7.20 Hz, 2H). LC/MS (APCI<sup>+</sup>): Calculated for C<sub>19</sub>H<sub>16</sub>Cl<sub>2</sub>N<sub>2</sub>O<sub>4</sub>S 439.31; Observed *m/z* [M+H]<sup>+</sup> 441.0. HPLC purity: 96%.

**3-(2,4-bis(4-chlorophenyl)thiazol-5-yl)-N-(methylsulfonyl)propanamide (57).—**

Yield: 20%. <sup>1</sup>H NMR (400 MHz, Methanol-*d*<sub>4</sub>) δ 7.98 – 7.90 (m, 2H), 7.73 – 7.62 (m, 2H), 7.55 – 7.45 (m, 4H), 3.29 (d, *J* = 7.2 Hz, 2H), 3.20 (s, 3H), 2.73 (t, *J* = 7.2 Hz, 2H). LC/MS (ESI<sup>+</sup>): Calculated for C<sub>19</sub>H<sub>16</sub>Cl<sub>2</sub>N<sub>2</sub>O<sub>3</sub>S 454.00; Observed *m/z* [M+H]<sup>+</sup> 455.0. HPLC purity: >99%.

**General procedure for the synthesis of carbamate 45 and ureas (42–44 and 58).:** To a solution of methanesulfonamide (1.5–2.5 equiv) in DCM or DMF was added DIPEA (7.5 equiv) and CDI (0.5–2.5 equiv) at 0 °C. The resulting mixture was stirred at 25 °C for 16 h. Then the appropriate amine or alcohol (1 equiv) dissolved in DCM or DMF (depending on

the solubility) was added and heated at 45 °C-90 °C for 24–48 h. Solvents were evaporated under reduced pressure. Crude product was purified by preparative HPLC or silica gel column chromatography.

***N*-(((3-(pyridin-4-yl)-1-(6-(trifluoromethyl)pyridin-3-yl)-1*H*-pyrazol-4-yl)methyl)carbamoyl)methanesulfonamide (42).**—Yield: 31%.

<sup>1</sup>H NMR (400 MHz, Methanol-*d*<sub>4</sub>) δ 9.35 (d, *J* = 2.36 Hz, 1H), 8.85 (d, *J* = 5.96 Hz, 2H), 8.66 (s, 1H), 8.56 (dd, *J* = 2.36, 8.42 Hz, 1H), 8.37 (d, *J* = 6.48 Hz, 2H), 8.02 (d, *J* = 8.60 Hz, 1H), 4.67 (s, 2H), 3.25 (s, 3H). LC/MS (APCI<sup>+</sup>): Calculated for C<sub>17</sub>H<sub>15</sub>F<sub>3</sub>N<sub>6</sub>O<sub>3</sub>S 440.40; Observed *m/z* [M+H]<sup>+</sup> 441.1.

***N*-(((1-(4-chlorophenyl)-3-(pyridin-4-yl)-1*H*-pyrazol-4-yl)methyl)carbamoyl)methanesulfonamide (43).**—Yield:

19%. <sup>1</sup>H NMR (400 MHz, Methanol-*d*<sub>4</sub>) δ 8.88 (d, *J* = 5.44 Hz, 2H), 8.53 (d, *J* = 5.20 Hz, 2H), 8.49 (s, 1H), 7.93 (d, *J* = 7.72 Hz, 2H), 7.58 (d, *J* = 7.72 Hz, 2H), 4.68 (s, 2H), 3.26 (s, 3H). <sup>13</sup>C NMR (151 MHz, Methanol-*d*<sub>4</sub>) δ 154.5, 149.8 (2C), 148.9, 143.7, 139.7, 133.7, 130.9, 130.7, 123.9, 123.7, 121.7, 121.5, 121.2, 120.6, 41.8, 35.5. LC/MS (APCI<sup>+</sup>): Calculated for C<sub>17</sub>H<sub>16</sub>ClN<sub>5</sub>O<sub>3</sub>S 405.86; Observed *m/z* [M+H]<sup>+</sup> 406.1; HPLC purity: 97%.

***N*-(((1,3-bis(4-chlorophenyl)-1*H*-pyrazol-4-yl)methyl)carbamoyl)methanesulfonamide (44).**—Yield:

15%. <sup>1</sup>H NMR (300 MHz, DMSO-*d*<sub>6</sub>) δ 10.00 (s, 1H), 8.51 (s, 1H), 7.94 – 7.88 (m, 2H), 7.80 – 7.74 (m, 2H), 7.63 – 7.53 (m, 4H), 6.85 (t, *J* = 5.4 Hz, 1H), 4.38 (d, *J* = 5.4 Hz, 2H), 3.22 (s, 3H). LC/MS (APCI<sup>+</sup>): Calculated for C<sub>18</sub>H<sub>16</sub>Cl<sub>2</sub>N<sub>4</sub>O<sub>3</sub>S 438.03; Observed *m/z* [M+H]<sup>+</sup> 438.9, 440.9; HPLC purity: 96%.

**(1-(4-chlorophenyl)-3-(pyridin-4-yl)-1*H*-pyrazol-4-yl)methyl (methylsulfonyl)carbamate (45).**—Yield: 26%. <sup>1</sup>H NMR (400 MHz, DMSO-*d*<sub>6</sub>) δ

11.81 (s, 1H), 8.81 (s, 1H), 8.71 (s, 2H), 7.95–7.98 (m, 2H), 7.79–7.80 (m, 2H), 7.62–7.64 (m, 2H), 5.29 (s, 2H), 3.24 (s, 3H). <sup>13</sup>C NMR (101 MHz, DMSO-*d*<sub>6</sub>) δ 152.4, 150.7, 150.5, 149.5, 139.7, 138.3, 132.0, 131.7, 130.1, 130.0 (2C), 122.3, 120.8, 120.5, 116.8, 58.4, 41.2. LC/MS (APCI<sup>+</sup>): Calculated for C<sub>17</sub>H<sub>15</sub>ClN<sub>4</sub>O<sub>4</sub>S 406.84; Observed *m/z* [M+H]<sup>+</sup> 407.1; HPLC purity: 98%.

***N*-(((5-(4-bromophenyl)-2-(pyridin-4-yl)furan-3-yl)methyl)carbamoyl)methanesulfonamide (58).**—Yield:

29%. <sup>1</sup>H NMR (400 MHz, DMSO-*d*<sub>6</sub>) δ 10.41 (s, 1H), 8.76 (d, *J* = 6.1 Hz, 2H), 8.00 (d, *J* = 6.1 Hz, 2H), 7.90 – 7.84 (m, 2H), 7.74 – 7.67 (m, 2H), 7.21 (s, 2H), 4.51 (d, *J* = 5.7 Hz, 2H), 3.24 (s, 3H). <sup>13</sup>C NMR (151 MHz, DMSO-*d*<sub>6</sub>) δ 158.2, 157.9, 153.5, 152.6, 146.0, 143.9, 140.1, 132.1 (2C), 129.9, 128.0, 126.3 (2C), 122.1, 119.9, 110.9, 41.4, 35.3. LC/MS (ESI<sup>+</sup>): Calculated C<sub>18</sub>H<sub>16</sub>BrN<sub>3</sub>O<sub>4</sub>S 449.00; Observed *m/z* [M+H]<sup>+</sup> 450.0, 452.0 (1:1) bromine isotopic pattern; HPLC purity: 96%.



**Synthesis of compounds with heterocyclic rings at C4 – 46–50.**

**5-(2-(1-(4-bromophenyl)-3-(4-chlorophenyl)-1*H*-pyrazol-4-yl)ethyl)-1*H*-tetrazole (46).**—To a solution of 3-(1-(4-bromophenyl)-3-(4-chlorophenyl)-1*H*-pyrazol-4-yl)propanenitrile (**93**) (100 mg, 258.62  $\mu\text{mol}$ ) in isopropanol (1 mL) and water (500  $\mu\text{L}$ ) was added  $\text{ZnBr}_2$  (58 mg, 258.62  $\mu\text{mol}$ , 13  $\mu\text{L}$ ) and  $\text{NaN}_3$  (50 mg, 775.86  $\mu\text{mol}$ , 27  $\mu\text{L}$ ) (Scheme S8). The mixture was stirred at 120 °C for 15 h. The reaction mixture was diluted with water (10 mL) and extracted with EtOAc (10 mL x 2). The combined organic layers were dried over  $\text{Na}_2\text{SO}_4$  and concentrated. The residue was purified by prep-HPLC (column: Phenomenex Synergi C18 150 $\times$ 30mm $\times$ 4 $\mu\text{m}$ ; mobile phase: [water (0.225%FA)-ACN]; B%: 60%-90%, 12min) to afford 5-(2-(1-(4-bromophenyl)-3-(4-chlorophenyl)-1*H*-pyrazol-4-yl)ethyl)-1*H*-tetrazole (**46**) as a white solid. Yield: 21 mg (19%).  $^1\text{H}$  NMR (300 MHz,  $\text{DMSO}-d_6$ )  $\delta$  8.52 (s, 1H), 7.85–7.83 (m, 2H), 7.77–7.70 (m, 4H), 7.56–7.54 (m, 2H), 3.22–3.18 (m, 2H), 3.12–3.10 (m, 2H). LC/MS (APCI $^+$ ): Calculated for  $\text{C}_{18}\text{H}_{14}\text{BrClN}_6$  428.02; Observed  $m/z$   $[\text{M}+\text{H}]^+$  429.0; HPLC purity: >99%.

**3-(2-(1-(4-bromophenyl)-3-(4-chlorophenyl)-1*H*-pyrazol-4-yl)ethyl)-1,2,4-oxadiazol-5(4*H*)-one (47).**

**Step 1.:** To a mixture of 3-(1-(4-bromophenyl)-3-(4-chlorophenyl)-1*H*-pyrazol-4-yl)propanenitrile (**93**) (1.00 g, 2.59 mmol) and  $\text{NH}_2\text{OH}\cdot\text{H}_2\text{O}$  (270 mg, 3.89 mmol) in water (5 mg, 259.00  $\mu\text{mol}$ ) and EtOH (10 mL) was added a solution of NaOMe (168 mg, 3.11 mmol) in MeOH (4 mL) (Scheme S8). The mixture was stirred at 90 °C for 6 h. The mixture was poured into water (10 mL) and stirred for 15 minutes. The solid was collected to afford (*Z*)-3-(1-(4-bromophenyl)-3-(4-chlorophenyl)-1*H*-pyrazol-4-yl)-*N*-hydroxypropanimidamide (**94**) as a light-yellow solid. Yield: 1 g (crude). LC/MS (APCI $^+$ ): Calculated for  $\text{C}_{18}\text{H}_{16}\text{BrClN}_4\text{O}$  418.02; Observed  $m/z$   $[\text{M}+\text{H}]^+$  419.0; HPLC purity: 69%.

**Step 2.:** To a solution of (*Z*)-3-(1-(4-bromophenyl)-3-(4-chlorophenyl)-1*H*-pyrazol-4-yl)-*N*-hydroxypropanimidamide (**94**) (250 mg, 411.01  $\mu\text{mol}$ ) in DMF (800  $\mu\text{L}$ ) and EtOH (2 mL) was added NaOMe (4 M, 206  $\mu\text{L}$ ). The mixture was stirred at 15 °C for 0.5 h and diethylcarbonate (304 mg, 2.57 mmol, 310  $\mu\text{L}$ ) was added. The mixture was stirred at 80 °C for another 16 h. The mixture was concentrated and diluted with water (5 mL). The aqueous phase was adjusted to pH=7 with 1 N HCl and extracted with EtOAc (5 mL x 3). The organic phase was concentrated and purified by prep-HPLC (column: Phenomenex Synergi C18 150 $\times$ 25 $\times$ 10 $\mu\text{m}$ ; mobile phase: [water (0.225%FA)-ACN]; B%: 65%-95%, 11min) to afford 3-(2-(1-(4-bromophenyl)-3-(4-chlorophenyl)-1*H*-pyrazol-4-yl)ethyl)-1,2,4-oxadiazol-5(4*H*)-one (**47**) as a white solid. Yield: 58 mg (32%).  $^1\text{H}$  NMR (400 MHz, Chloroform-*d*)  $\delta$  9.41 (s, 1H), 7.86 (s, 1H), 7.66–7.54 (m, 6H), 7.47–7.40 (m, 2H), 3.17–3.02 (m, 2H), 2.88–2.77 (m, 2H). LC/MS (APCI $^+$ ): Calculated for  $\text{C}_{19}\text{H}_{14}\text{BrClN}_4\text{O}_2$  444.00; Observed  $m/z$   $[\text{M}+\text{H}]^+$  445.0; HPLC purity: >99%.

**5-((1,3-bis(4-chlorophenyl)-1*H*-pyrazol-4-yl)methyl)pyrimidine-2,4,6(1*H*,3*H*,5*H*)-trione (48).**—To a solution of 1,3-bis(4-chlorophenyl)-1*H*-pyrazole-4-carbaldehyde (**61h**) (0.150 g, 0.473 mmol) and pyrimidine-2,4,6(1*H*,3*H*,5*H*)-trione (0.064 g, 0.500 mmol) in a mixture of EtOH (10 mL) and DMF (10 mL) (Scheme S9). The reaction mixture was heated in a pressure tube to 80 °C for 16 h. The resulting suspension was cooled

to 25 °C, NaBH<sub>4</sub> (0.038 g, 1.004 mmol) was added and the resulting reaction was stirred for 1 h at 25 °C to yield a clear orange solution. The solvents were evaporated *in vacuo* to afford a residue. To the obtained residue were added water (80 mL) and some NaCl and hexane (70 mL) and EtOAc (10 mL) and the resulting suspension was acidified with HCl to pH = 2 and stirred for 1 h. The resulting precipitate was filtered off, yielding a white solid. The water layer was reextracted with EtOAc (80 mL x 2), and the combined organic phases were dried over Na<sub>2</sub>SO<sub>4</sub>, evaporated and purified by SiO<sub>2</sub> flash chromatography [CH<sub>2</sub>Cl<sub>2</sub>/iPrOH 95/5 to 90/10], yielding 5-((1,3-*bis*(4-chlorophenyl)-1*H*-pyrazol-4-yl)methyl)-5-hydroxypyrimidine-2,4,6-(1*H*,3*H*,5*H*)-trione (0.027 g, 0.059 mmol, 12%) as a slightly yellowish solid (by-product). The white precipitate showed broad signals in the NMR [due to B(OH)<sub>3</sub> contamination] and was therefore dissolved in MeOH (80 mL) and HCl conc (1 mL) and the solvent was evaporated. This procedure was repeated, to give 5-((1,3-*bis*(4-chlorophenyl)-1*H*-pyrazol-4-yl)methyl)pyrimidine-2,4,6-(1*H*,3*H*,5*H*)-trione (**48**) as a yellow solid. Yield: 162 mg (78%). <sup>1</sup>H NMR (300 MHz, DMSO-*d*<sub>6</sub>) δ 11.77 (s, 2H), 8.18 (s, 1H), 7.86 (d, *J* = 8.8 Hz, 2H), 7.69 (d, *J* = 8.4 Hz, 2H), 7.57 (d, *J* = 8.8 Hz, 2H), 7.53 (d, *J* = 8.4 Hz, 2H), 3.66 (s, 2H), 3.39 (s, 1H). LC/MS (ESI<sup>+</sup>): Calculated for C<sub>20</sub>H<sub>14</sub>Cl<sub>2</sub>N<sub>4</sub>O<sub>3</sub> 428.04; Observed *m/z* [M+H]<sup>+</sup> 429.1, 431.0; HPLC purity: 98%.

**5-(2-(1-(4-bromophenyl)-3-(4-chlorophenyl)-1*H*-pyrazol-4-yl)ethyl)-1,3,4-oxadiazol-2(3*H*)-one (**49**).**

**Step 1.:** The reaction mixture of 3-(1-(4-bromophenyl)-3-(4-chlorophenyl)-1*H*-pyrazol-4-yl)propanoic acid (**26**) (500 mg, 1.23 mmol), Et<sub>3</sub>N (36 mg, 356.70 μmol, 49 μL) and NH<sub>2</sub>NH<sub>2</sub>·H<sub>2</sub>O (157 mg, 3.08 mmol, 153 μL) in toluene was stirred at 130 °C for 3 h (Scheme S8). The mixture was separated between water (3 mL) and EtOAc (3 mL). The aqueous phase was extracted with EtOAc (3 mL x 2). The combined organic phase was washed with brine (5 mL), dried with anhydrous Na<sub>2</sub>SO<sub>4</sub>, filtered and concentrated to afford crude 3-(1-(4-bromophenyl)-3-(4-chlorophenyl)-1*H*-pyrazol-4-yl)propanehydrazide (**95**) as a yellow solid. Yield: 250 mg (48%). LC/MS (APCI<sup>+</sup>): Calculated for C<sub>18</sub>H<sub>16</sub>BrClN<sub>4</sub>O 418.02; Observed *m/z* [M+H]<sup>+</sup> 419.0; HPLC purity: 67%.

**Step 2.:** To the solution of 3-(1-(4-bromophenyl)-3-(4-chlorophenyl)-1*H*-pyrazol-4-yl)propanehydrazide (**95**) (250 mg, 595.66 μmol) in THF (5 mL) was added CDI (145 mg, 893.49 μmol). The mixture was stirred at 60 °C for 4 h under nitrogen atmosphere. The mixture was poured into water (5 mL) and extracted with EtOAc (10 mL x 3). The organic phase was concentrated and purified by prep-HPLC (column: Phenomenex Synergi C18 150×25×10μm; mobile phase: [water (0.225%FA)-ACN]; B%: 65%-95%, 10min) to afford 5-(2-(1-(4-bromophenyl)-3-(4-chlorophenyl)-1*H*-pyrazol-4-yl)ethyl)-1,3,4-oxadiazol-2(3*H*)-one (**49**) as a white solid. Yield: 93 mg (34%). <sup>1</sup>H NMR (300 MHz, DMSO-*d*<sub>6</sub>) δ 8.57 (s, 1H), 7.86–7.82 (m, 2H), 7.76–7.69 (m, 4H), 7.59–7.51 (m, 2H), 3.05–2.96 (m, 2H), 2.94–2.87 (m, 2H). LC/MS (APCI<sup>+</sup>): Calculated for C<sub>19</sub>H<sub>14</sub>BrClN<sub>4</sub>O<sub>2</sub> 444.00; Observed *m/z* [M+H]<sup>+</sup> 445.0; HPLC purity: 98%.

***N*-(5-(1,3-*bis*(4-chlorophenyl)-1*H*-pyrazol-4-yl)-4,5-dihydroisoxazol-3-yl)methanesulfonamide (**50**).**—To a solution of methanesulfonamide

(250 mg, 2.63 mmol) in DMF (2 mL) was added NaH (100 mg, 2.71 mmol) and the reaction mixture was stirred for 3 min under nitrogen atmosphere. Then a solution of 5-(1,3-*bis*(4-chlorophenyl)-1*H*-pyrazol-4-yl)-3-bromo-4,5-dihydroisoxazole (**97**) (0.100 g, 0.229 mmol) in DMF (2 mL) was added and the mixture was heated to 90 °C in a pressure tube for 16 h (Scheme S9). The cooled solution was diluted with NaHCO<sub>3</sub> solution (50 mL) and extracted with EtOAc (2 × 50 mL). The organic phase was dried over Na<sub>2</sub>SO<sub>4</sub>, evaporated and the material was purified by flash chromatography (Et<sub>2</sub>O/HCOOH 99.5/0.5 to 99/1) yielding *N*-(5-(1,3-*bis*(4-chlorophenyl)-1*H*-pyrazol-4-yl)-4,5-dihydroisoxazol-3-yl)methanesulfonamide (**50**) after crystallization from CH<sub>2</sub>Cl<sub>2</sub>/diisopropylether. Yield: 28 mg (27%). <sup>1</sup>H NMR (300 MHz, Methanol-*d*<sub>4</sub>) δ 8.50 (s, 1H), 7.86 (d, *J* = 9.0 Hz, 2H), 7.80 (d, *J* = 8.6 Hz, 2H), 7.55–7.47 (m, 4H), 5.71 (t, *J* = 10.0 Hz, 1H), 3.47 (dd, *J* = 16.7, 9.8 Hz, 1H), 3.31 – 3.24 (m, 1H), 3.21 (s, 3H). LC/MS (ESI<sup>+</sup>): Calculated for C<sub>19</sub>H<sub>16</sub>Cl<sub>2</sub>N<sub>4</sub>O<sub>3</sub>S 450.03; Observed *m/z* [M+H]<sup>+</sup> 450.8, 452.8; HPLC purity: >99%.

## Supplementary Material

Refer to Web version on PubMed Central for supplementary material.

## ACKNOWLEDGMENT

DuPont Chemicals, USA for donating the compound library. Dr. Sridevi Bashayam, Dr. Jayanth Thiruvellore, and Mr. Rajkumar Dhinakaran, from Syngene, India and the chemistry team from WuXi AppTec, China for profound chemistry support. Tando Ntsabo and Nicole Cardoso from TB biology, H3D for performing MIC and biology triage assays. Technical staff at *in vitro* DMPK and parasitology divisions of H3D for excellent technical assistance in generating all *in vitro* DMPK and cytotoxicity data, Marianna de Kock and Claudia Spies, SAMRC and Stellenbosch University, South Africa for excellent technical assistance in generating MICs against clinical TB isolates.

## Funding Sources

The project was funded through Global Health Grants (Number OPP1066878) received from the Bill and Melinda Gates Foundation, the Division of Intramural Research of the NIAID/ NIH, and the Strategic Health Innovation Partnerships (SHIP) unit of the South African Medical Research Council (SAMRC). The University of Cape Town, SAMRC, and South African Research Chairs Initiative of the Department of Science and Innovation, administered through the South African National Research Foundation are gratefully acknowledged for support (K.C.).

## ABBREVIATIONS

<b>TB</b>	tuberculosis
<b>MIC</b>	minimum inhibitory concentration
<b>SAR</b>	structure-activity relationship
<b>RT</b>	room temperature
<b>MeOH</b>	methanol
<b>EtOH</b>	ethanol
<b>EtOAc</b>	ethyl acetate
<b>DIPEA</b>	diisopropylethylamine

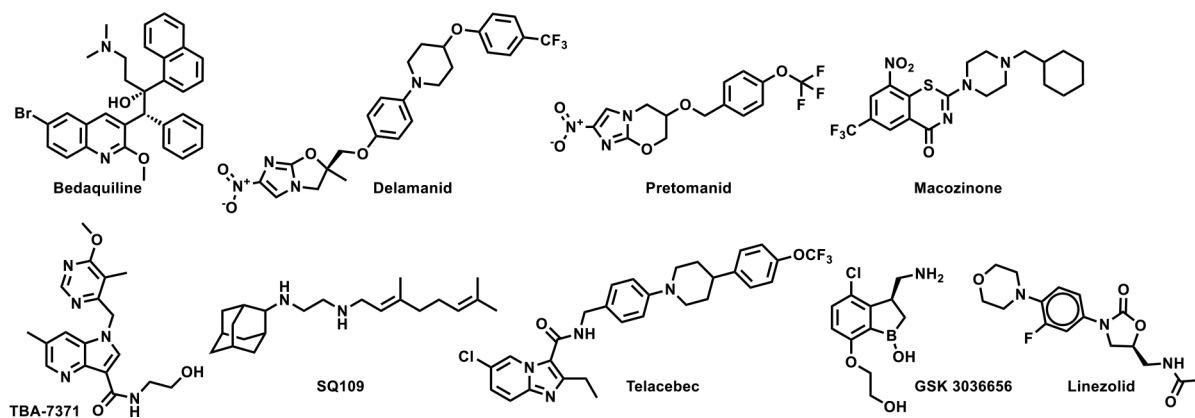
<b>THF</b>	tetrahydrofuran
<b>DMF</b>	<i>N,N</i> -dimethylformamide
<b>BuOH</b>	butanol
<b>HATU</b>	1-[Bis(dimethylamino)methylene]-1 <i>H</i> -1,2,3-triazolo[4,5- <i>b</i> ]pyridinium 3-oxid hexafluorophosphate
<b>POCl<sub>3</sub></b>	Phosphorus(V) oxychloride
<b>SOCl<sub>2</sub></b>	thionyl chloride
<b>NaBH<sub>4</sub></b>	sodium borohydride
<b>NaCNBH<sub>3</sub></b>	Sodium cyanoborohydride
<b>LAH</b>	lithium aluminum hydride
<b>mCPBA</b>	meta-chloroperbenzoic acid
<b>AUC</b>	area under the curve

## REFERENCES

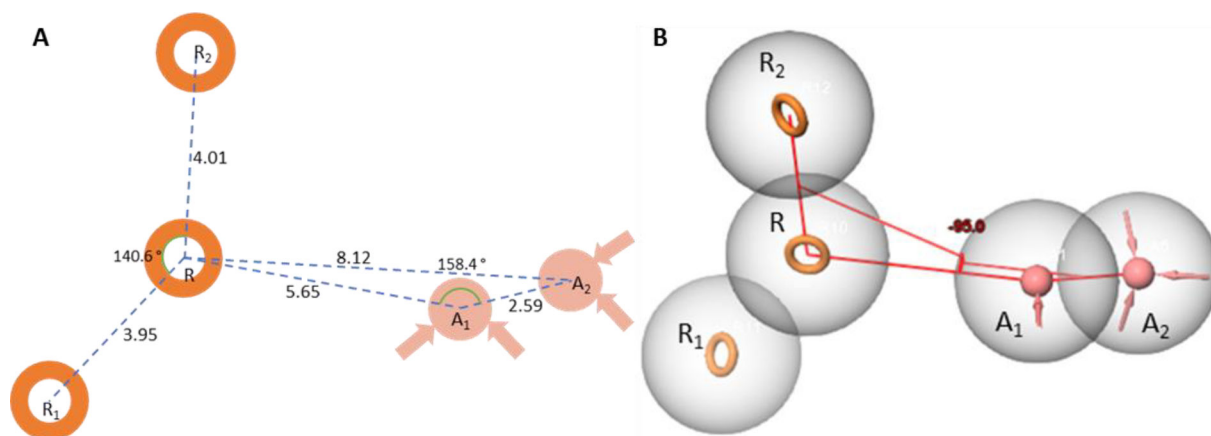
1. World Health Organization Global Tuberculosis Report 2019. <https://www.who.int/tb/global-report-2019> (2020-08-13).
2. Pontali E; Sotgiu G; D' Ambrosio L; Centis R; Migliori GB Bedaquiline and multidrug-resistant tuberculosis: A systematic and critical analysis of the evidence. *European Respiratory Journal* 2016, 47, 394–402. [PubMed: 26828052]
3. Our Pipeline: Pretomanid. <https://www.tballiance.org/portfolio/compound/pretomanid> (April 19, 2021).
4. Xavier A; Lakshmanan M Delamanid: A new armor in combating drug-resistant tuberculosis. *Journal of Pharmacology and Pharmacotherapeutics* 2014, 5, 222–224. [PubMed: 25210407]
5. Makarov V; Mikušová K Development of Macozinone for TB treatment: An update. *Applied Sciences* 2020, 10, 2269.
6. Early bactericidal activity of TBA-7371 in pulmonary tuberculosis. <https://clinicaltrials.gov/ct2/show/NCT04176250>
7. Sacksteder KA; Protopopova M; Barry CE; Andries K; Nacy CA Discovery and development of SQ109: A new antitubercular drug with a novel mechanism of action. *Future Microbiology* 2012, 7, 823–837. [PubMed: 22827305]
8. de Jager VR; Dawson R; van Niekerk C; Hutchings J; Kim J; Vanker N; van der Merwe L; Choi J; Nam K; Diacon AH Telacebec (Q203), a new antituberculosis agent. *New England Journal of Medicine* 2020, 382, 1280–1281. [PubMed: 32212527]
9. Tenero D; Derimanov G; Carlton A; Tonkyn J; Davies M; Cozens S; Gresham S; Gaudion A; Puri A; Muliaditan M; Rullas-Trincado J; Mendoza-Losana A; Skingsley A; Barros-Aguirre D First-time-in-human study and prediction of early bactericidal activity for GSK3036656, a potent leucyl-tRNA synthetase inhibitor for tuberculosis treatment. *Antimicrobial Agents and Chemotherapy* 2019, 63, e00240–19. [PubMed: 31182528]
10. Schechter GF; Scott C; True L; Raftery A; Flood J; Mase S Linezolid in the treatment of multidrug-resistant tuberculosis. *Clinical Infectious Diseases* 2010, 50, 49–55. [PubMed: 19947856]
11. Niederweis M Nutrient acquisition by mycobacteria. *Microbiology* 2008, 154, 679–692. [PubMed: 18310015]

12. Warner DF Mycobacterium tuberculosis metabolism. Cold Spring Harbor Perspectives in Medicine 2015, 5.
13. Wilburn KM; Fieweger RA; VanderVen BC Cholesterol and fatty acids grease the wheels of Mycobacterium tuberculosis pathogenesis. Pathogens and Disease 2018, 76.
14. Brzostek A; Pawelczyk J; Rumijowska-Galewicz A; Dziadek B; Dziadek J Mycobacterium tuberculosis is able to accumulate and utilize cholesterol. Journal of Bacteriology 2009, 191, 6584–6591. [PubMed: 19717592]
15. Marrero J; Trujillo C; Rhee KY; Ehrt S Glucose phosphorylation is required for Mycobacterium tuberculosis persistence in mice. PLOS Pathogens 2013, 9, e1003116. [PubMed: 23326232]
16. Martinez-Grau MA; Valcarcel ICG; Early JV; Gessner RK; de Melo CS; de la Nava EMM; Korkegian A; Ovechkina Y; Flint L; Gravelle A; Cramer JW; Desai PV; Street LJ; Odingo J; Masquelin T; Chibale K; Parish T Synthesis and biological evaluation of aryl-oxadiazoles as inhibitors of Mycobacterium tuberculosis. Bioorganic & Medicinal Chemistry Letters 2018, 28, 1758–1764. [PubMed: 29680666]
17. Gold B; Pingle M; Brickner SJ; Shah N; Roberts J; Rundell M; Bracken WC; Warriar T; Somersan S; Venugopal A; Darby C; Jiang X; Warren JD; Fernandez J; Ouerfelli O; Nuermberger EL; Cunningham-Bussel A; Rath P; Chidawanyika T; Deng H; Realubit R; Glickman JF; Nathan CF Nonsteroidal anti-inflammatory drug sensitizes Mycobacterium tuberculosis to endogenous and exogenous antimicrobials. Proceedings of the National Academy of Sciences 2012, 109, 16004–16011.
18. Salunke SB; Azad AK; Kapuriya NP; Balada-Llasat JM; Pancholi P; Schlesinger LS; Chen CS Design and synthesis of novel anti-tuberculosis agents from the celecoxib pharmacophore. Bioorg Med Chem 2015, 23, 1935–43. [PubMed: 25818768]
19. Yadlapalli RK; Chourasia OP; Vemuri K; Sritharan M; Perali RS Synthesis and in vitro anticancer and antitubercular activity of diarylpyrazole ligated dihydropyrimidines possessing lipophilic carbamoyl group. Bioorg Med Chem Lett 2012, 22, 2708–11. [PubMed: 22437116]
20. Nardi A.-n.; Christensen J.; Kejser; Jones D, Spencer. Novel pyrazole derivatives useful as potassium channel modulators. WO 2009/003921 A1, 08.01.2009, 2008.
21. Swiss R; Will Y Assessment of mitochondrial toxicity in HepG2 cells cultured in high-glucose- or galactose-containing media. Current Protocols in Toxicology 2011, 49, 2.20.1–2.20.14.
22. Dixon SL; Smondyrev AM; Knoll EH; Rao SN; Shaw DE; Friesner RA PHASE: A new engine for pharmacophore perception, 3D QSAR model development, and 3D database screening: 1. Methodology and preliminary results. Journal of Computer-Aided Molecular Design 2006, 20, 647–671. [PubMed: 17124629]
23. ACD/Labs, Release 2019.2.2, Advanced Chemistry Development, Inc. In Toronto, Ontario, Canada, 2020.
24. Arora K; Ochoa-Montano B; Tsang PS; Blundell TL; Dawes SS; Mizrahi V; Bayliss T; Mackenzie CJ; Cleghorn LAT; Ray PC; Wyatt PG; Uh E; Lee J; Barry CE; Boshoff HI Respiratory flexibility in response to inhibition of cytochrome oxidase in Mycobacterium tuberculosis. Antimicrobial Agents and Chemotherapy 2014, 58, 6962–6965. [PubMed: 25155596]
25. Moosa A; Lamprecht DA; Arora K; Barry CE; Boshoff HIM; Ioerger TR; Steyn AJC; Mizrahi V; Warner DF Susceptibility of Mycobacterium tuberculosis cytochrome oxidase mutants to compounds targeting the terminal respiratory oxidase, cytochrome c. Antimicrobial Agents and Chemotherapy 2017, 61, e01338–17. [PubMed: 28760899]
26. Naran K; Moosa A; Barry CE; Boshoff HIM; Mizrahi V; Warner DF Bioluminescent reporters for rapid mechanism of action assessment in tuberculosis drug discovery. Antimicrobial Agents and Chemotherapy 2016, 60, 6748–6757. [PubMed: 27572410]
27. Ardito F; Posteraro B; Sanguinetti M; Zanetti S; Fadda G Evaluation of BACTEC Mycobacteria Growth Indicator Tube (MGIT 960) automated system for drug susceptibility testing of Mycobacterium tuberculosis. Journal of Clinical Microbiology 2001, 39, 4440–4444. [PubMed: 11724858]
28. Rowland M Protein binding and drug clearance. Clinical Pharmacokinetics 1984, 9, 10–17. [PubMed: 6705422]

29. Varma MVS; Chang G; Lai Y; Feng B; El-Kattan AF; Litchfield J; Goosen TC Physicochemical property space of hepatobiliary transport and computational models for predicting rat biliary excretion. *Drug Metabolism and Disposition* 2012, 40, 1527–1537. [PubMed: 22580868]
30. Smith DA Evolution of ADME science: Where else can modeling and simulation contribute? *Molecular Pharmaceutics* 2013, 10, 1162–1170. [PubMed: 23294153]
31. Gao W; Kim J-Y; Anderson JR; Akopian T; Hong S; Jin Y-Y; Kandror O; Kim J-W; Lee I-A; Lee S-Y; McAlpine JB; Mulugeta S; Sunoqrot S; Wang Y; Yang S-H; Yoon T-M; Goldberg AL; Pauli GF; Suh J-W; Franzblau SG; Cho S The cyclic peptide ecumicin targeting ClpC1 is active against *Mycobacterium tuberculosis* in vivo. *Antimicrobial Agents and Chemotherapy* 2015, 59, 880–889. [PubMed: 25421483]
32. Cho SH; Warit S; Wan B; Hwang CH; Pauli GF; Franzblau SG Low-oxygen-recovery assay for high-throughput screening of compounds against nonreplicating *Mycobacterium tuberculosis*. *Antimicrobial Agents and Chemotherapy* 2007, 51, 1380–1385. [PubMed: 17210775]
33. Akester JN; Njaria P; Nchinda A; Le Manach C; Myrick A; Singh V; Lawrence N; Njoroge M; Taylor D; Moosa A; Smith AJ; Brooks EJ; Lenaerts AJ; Robertson GT; Ioerger TR; Mueller R; Chibale K Synthesis, structure–activity relationship, and mechanistic studies of aminoquinazolinones displaying antimycobacterial activity. *ACS Infectious Diseases* 2020, 6, 1951–1964. [PubMed: 32470286]
34. Ray PC; Huggett M; Turner PA; Taylor M; Cleghorn LAT; Early J; Kumar A; Bonnett SA; Flint L; Joerss D; Johnson J; Korkegian A; Mullen S; Moure AL; Davis SH; Murugesan D; Mathieson M; Caldwell N; Engelhart CA; Schnappinger D; Epemolu O; Zuccotto F; Riley J; Scullion P; Stojanovski L; Massoudi L; Robertson GT; Lenaerts AJ; Freiberg G; Kempf DJ; Masquelin T; Hipskind PA; Odingo J; Read KD; Green SR; Wyatt PG; Parish T Spirocyclic MmpL3 inhibitors with improved hERG and cytotoxicity profiles as inhibitors of *Mycobacterium tuberculosis* growth. *ACS Omega* 2021, 6, 2284–2311. [PubMed: 33521468]
35. Oh S; Park Y; Engelhart CA; Wallach JB; Schnappinger D; Arora K; Manikkam M; Gac B; Wang H; Murgolo N; Olsen DB; Goodwin M; Sutphin M; Weiner DM; Via LE; Boshoff HIM; Barry CE Discovery and structure–activity-relationship study of N-alkyl-5-hydroxypyrimidinone carboxamides as novel antitubercular agents targeting decaprenylphosphoryl- $\beta$ -d-ribose 2'-oxidase. *Journal of Medicinal Chemistry* 2018, 61, 9952–9965. [PubMed: 30350998]
36. Singh V; Donini S; Pacitto A; Sala C; Hartkoorn RC; Dhar N; Keri G; Ascher DB; Mondésert G; Vocat A; Lupien A; Sommer R; Vermet H; Lagrange S; Buechler J; Warner DF; McKinney JD; Pato J; Cole ST; Blundell TL; Rizzi M; Mizrahi V The inosine monophosphate dehydrogenase, Guab2, is a vulnerable new bactericidal drug target for tuberculosis. *ACS Infectious Diseases* 2017, 3, 5–17. [PubMed: 27726334]
37. Boshoff HIM; Myers TG; Copp BR; McNeil MR; Wilson MA; Barry CE The transcriptional responses of *Mycobacterium tuberculosis* to inhibitors of metabolism: Novel insights into drug mechanisms of action. *Journal of Biological Chemistry* 2004, 279, 40174–40184. [PubMed: 15247240]
38. Schrödinger Release 2020–2: Maestro, Schrodinger2020–2: New York, NY, 2020.

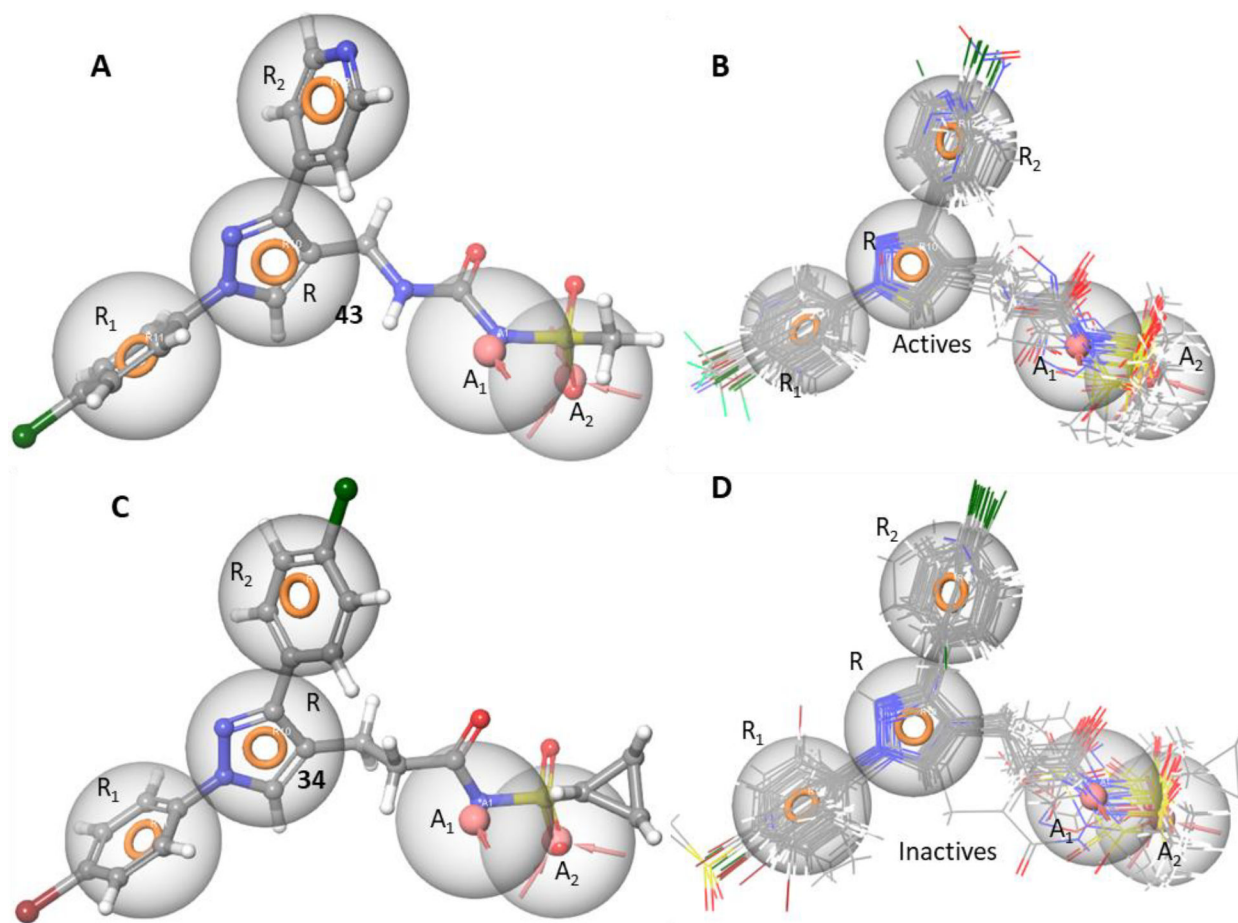


**Figure 1.**  
New approved drugs and clinical candidate for TB



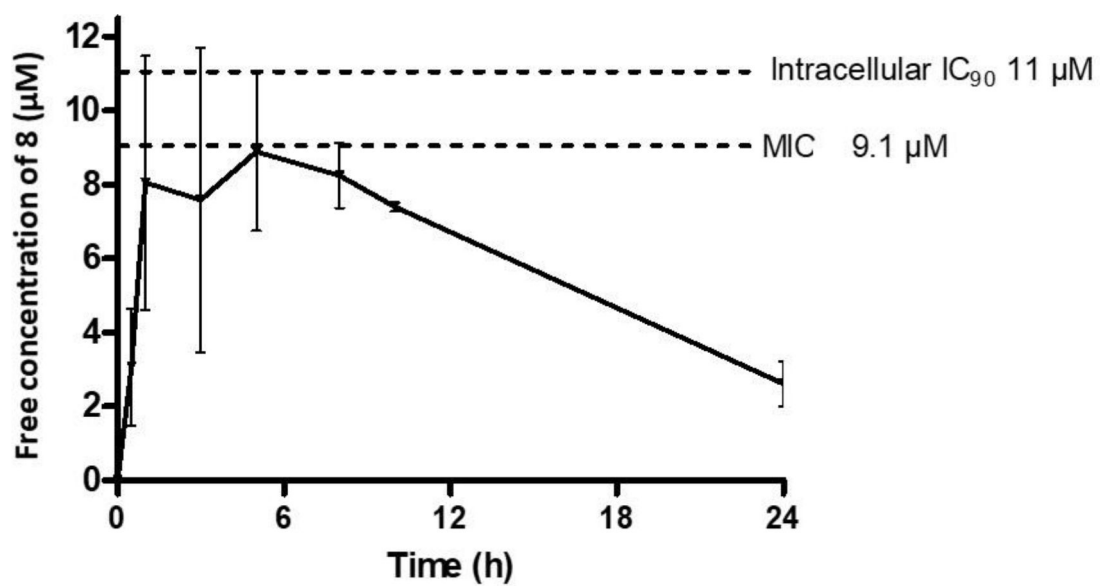
**Figure 2:** Representations of the AARRR pharmacophore model. A) A 2D representation of the pharmacophore model with two of the ring features (R<sub>1</sub> and R<sub>2</sub>) both shown to be about 4 Å from the central R feature forming an angle of 140° with each other. The first acceptor feature (A<sub>1</sub>) lies 5.65 Å from R with the acceptor feature A<sub>2</sub> lying an additional 2.59 Å from A<sub>1</sub> forming an angle of 158.4° with A<sub>1</sub> and R. B) A 3D representation of the pharmacophore model showing the A<sub>1</sub> and A<sub>2</sub> features to be out of the plane formed by R, R<sub>1</sub> and R<sub>2</sub> with a -95.0° dihedral angle around a line from R to A<sub>1</sub>.



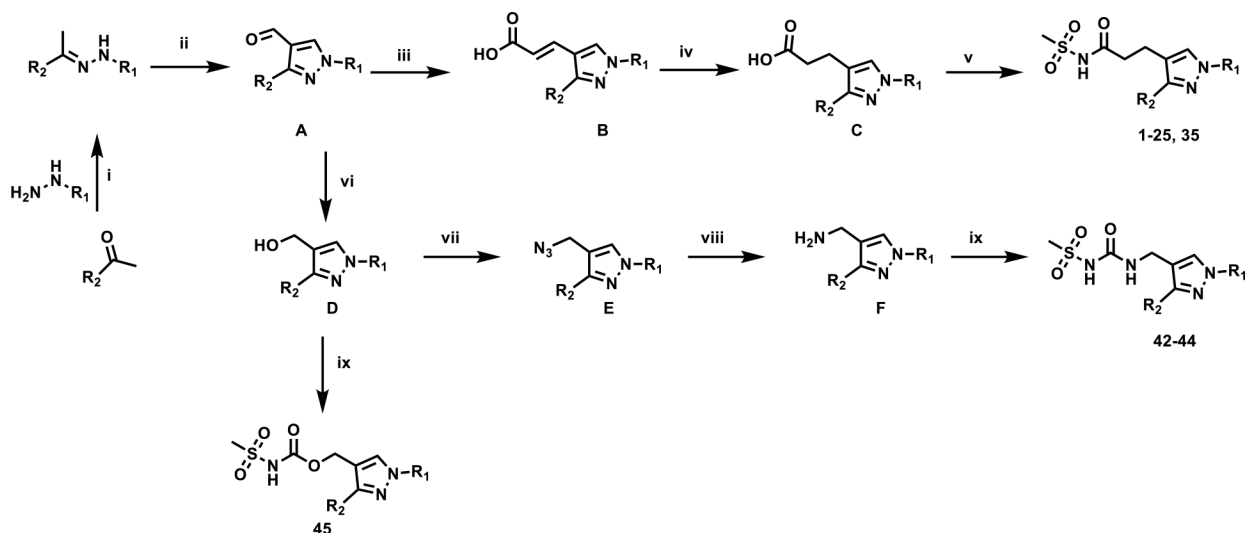


**Figure 3.**

A) Compound **43** fitted to the 5-feature AARRR pharmacophore hypothesis very closely. The three aromatic ring features are occupied by the chlorophenyl, pyrazole and pyridyl groups while the deprotonated sulfonamide fits the negative charge feature, and a sulfone O fits the acceptor feature; B) An overlay of all the active compounds in this set closely fitting all the five pharmacophore features. C) Compound **34** is an example of an inactive compound that is an excellent fit of the pharmacophore. This loss in activity is brought about by the bulky cyclopropyl group extending into a region outside of the pharmacophore. This region could be defined as an excluded volume. D) The inactive compounds from this set either fit the pharmacophore hypothesis fully or partially with many occupying spaces outside the definition of the pharmacophore suggesting potential for the definition of excluded volumes past the A<sub>2</sub> feature and between the A<sub>1</sub> and R<sub>1</sub> features.



**Figure 4.** Free exposures of **8** (calculated using human PPB) following a single oral dose of 200 mg/kg in mice.

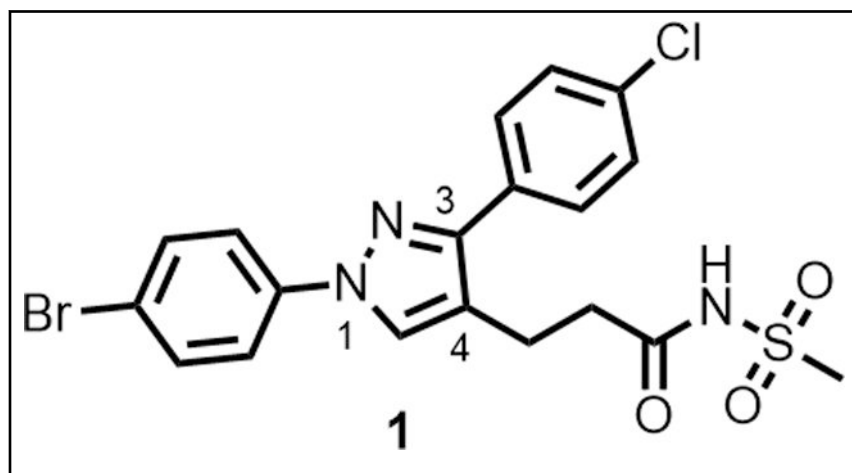


### Scheme 1. General synthetic scheme

Reagents and conditions: (i) KOAc, EtOH, 80 °C; (ii) POCl<sub>3</sub>, DMF, 80 °C; (iii) Malonic acid, piperidine, pyridine, 90 °C; (iv) method 1: NH<sub>2</sub>NH<sub>2</sub>.H<sub>2</sub>O, MeOH, 80 °C; method 2: NBSH, Et<sub>3</sub>N, THF, 45 °C; (v) method 1: CH<sub>3</sub>SO<sub>2</sub>NH<sub>2</sub>, CDI, DBU, DMF, 90 °C, method 2: CH<sub>3</sub>SO<sub>2</sub>NH<sub>2</sub>, DCC, DMAP, 0 – 45 °C; (vi) NaBH<sub>4</sub>, MeOH, 25 °C; (vii) PPh<sub>3</sub>, DIAD, NaN<sub>3</sub>, H<sub>2</sub>SO<sub>4</sub>, DCM, 0 °C to 25 °C; (viii) PPh<sub>3</sub>, THF/H<sub>2</sub>O, 60 °C; (ix) CDI, methanesulfonyl chloride, DIPEA, DCM, DCE or DMF depending on the solubility of the substrate, 25 °C – 90 °C.

Table 1.

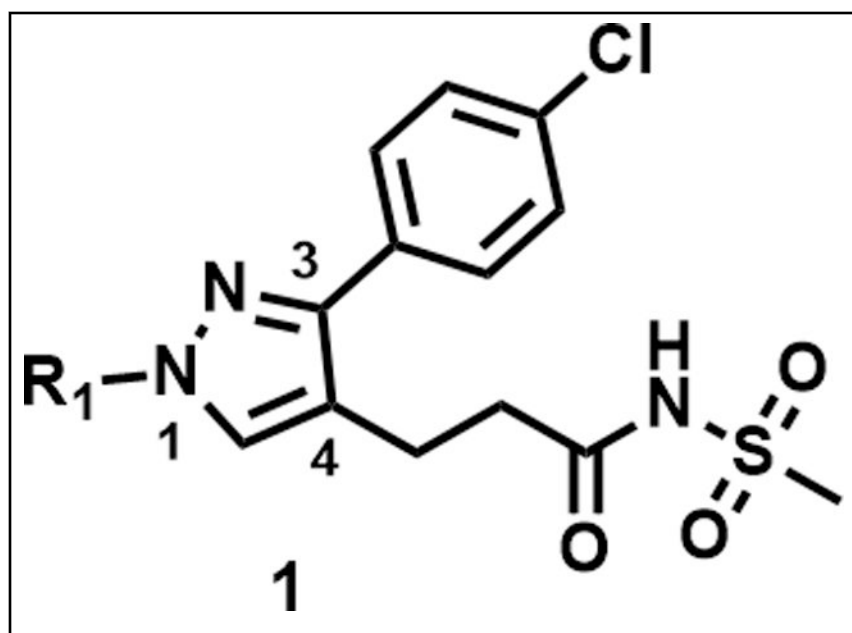
Hit triage of compound 1

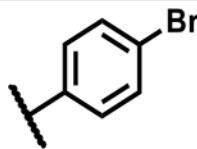
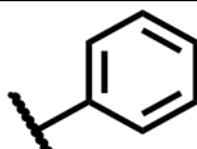
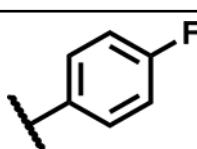
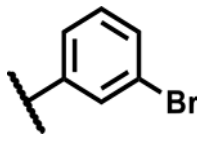


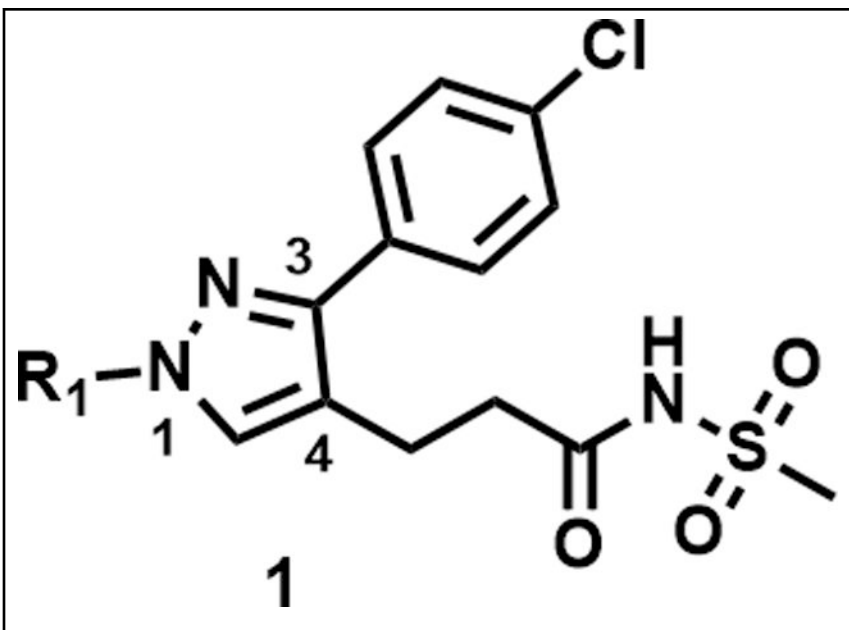
MIC 7H9/ADC/Tw ( $\mu\text{M}$ )	4.7
MIC 7H9/glucose/BSA/Tx ( $\mu\text{M}$ )	4.7
MIC 7H9/DPPC/cholesterol/BSA/Tx ( $\mu\text{M}$ )	4.7
MIC 7H9/cholesterol/BSA/Tx ( $\mu\text{M}$ )	4.7
IC <sub>90</sub> in 7H9/2.5mM butyrate/pH6/0.1mM nitrite ( $\mu\text{M}$ )	6.25
HepG2 IC <sub>50</sub> glucose ( $\mu\text{M}$ )	>50
HepG2 IC <sub>50</sub> galactose ( $\mu\text{M}$ )	>50
Solubility ( $\mu\text{M}$ )	170

MIC - minimum inhibitory concentration against *Mtb* H37Rv; 7H9 - Middlebrook 7H9; ADC - Albumin-Dextrose-Catalase supplement; Tw - Tween 80; BSA - Bovine serum albumin; Tx - Tyloxapol; DPPC - Dipalmitoylphosphatidylcholine and cholesterol; IC<sub>50</sub> - 50% inhibitory concentration; Solubility - Aqueous Solubility at pH 7.4

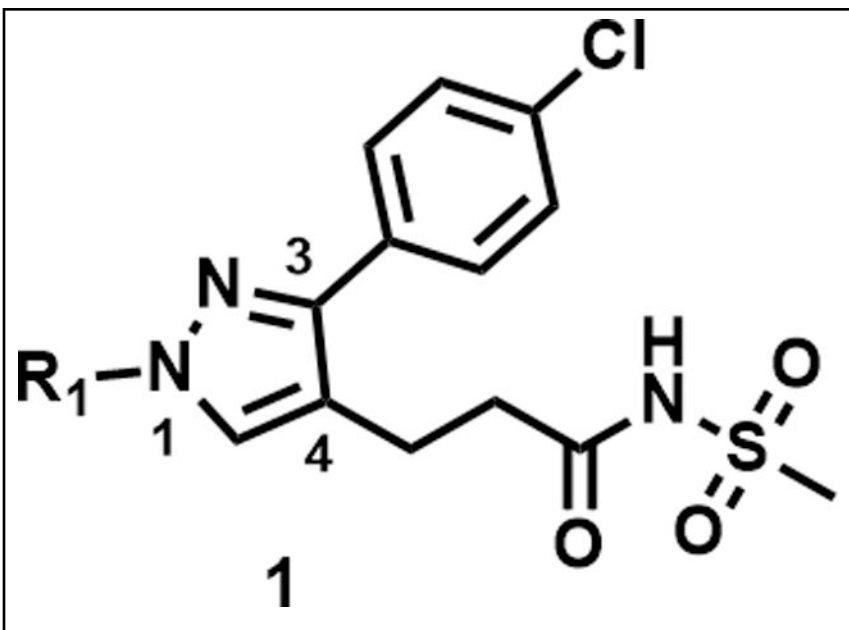
Table 2.

SAR at the *M1*-substituent


Compound Number	R <sub>1</sub>	MIC (μM)	Solubility (μM)
1		4.7	170
2		>50	200
3		37	25
4		>50	<5



Compound Number	R <sub>1</sub>	MIC (μM)	Solubility (μM)
5		>50	165
6		>50	190
7		>50	200
8		4.7	100

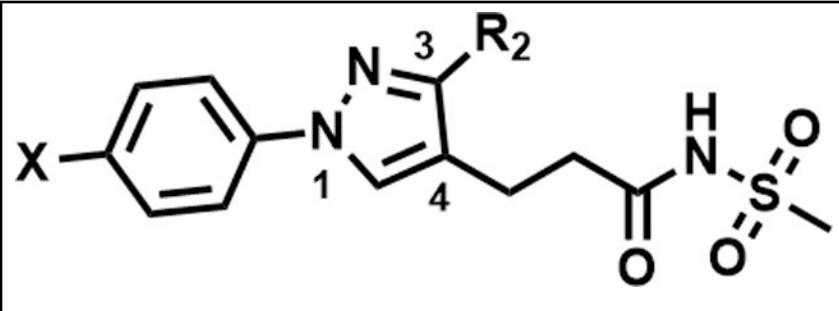


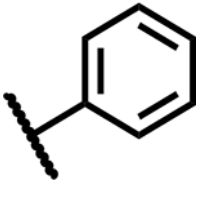
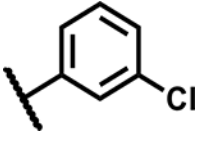
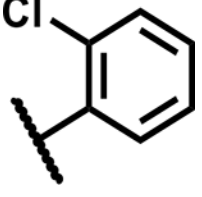
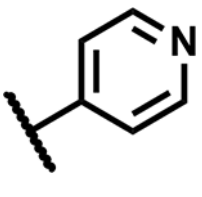
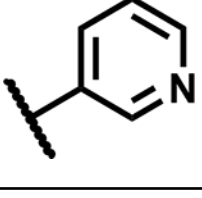
Compound Number	R <sub>1</sub>	MIC (μM)	Solubility (μM)
9		3.1	50
10		4.7	90
11		25	75
12		50	200

MICs were measured in Middlebrook 7H9/Glu/BSA/Tyloxapol media; Solubility was determined in aqueous pH 7.4 phosphate buffer simulating thermodynamic conditions.

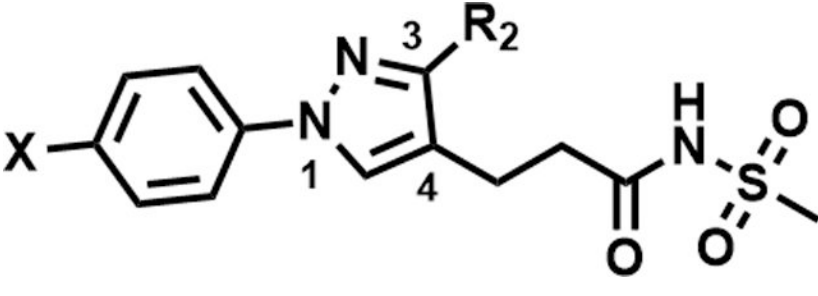
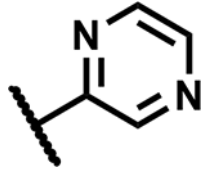
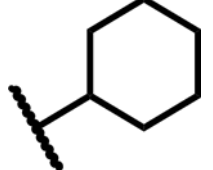
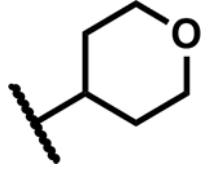
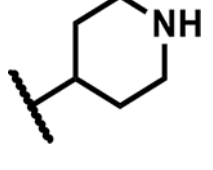
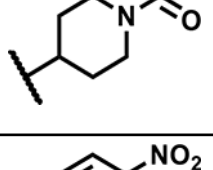
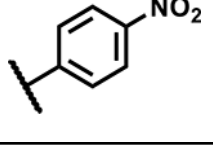
Table 3.

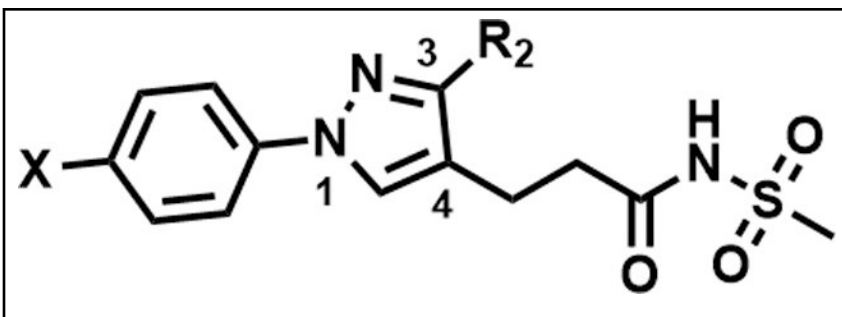
SAR at C3-position



Compound Number	X	R <sub>2</sub>	MIC (μM)	Solubility (μM)
13	Br		2.3	200
14	Br		2.3	165
15	Cl		>50	90
16	Br		1.2	185
17	Br		6.25	200



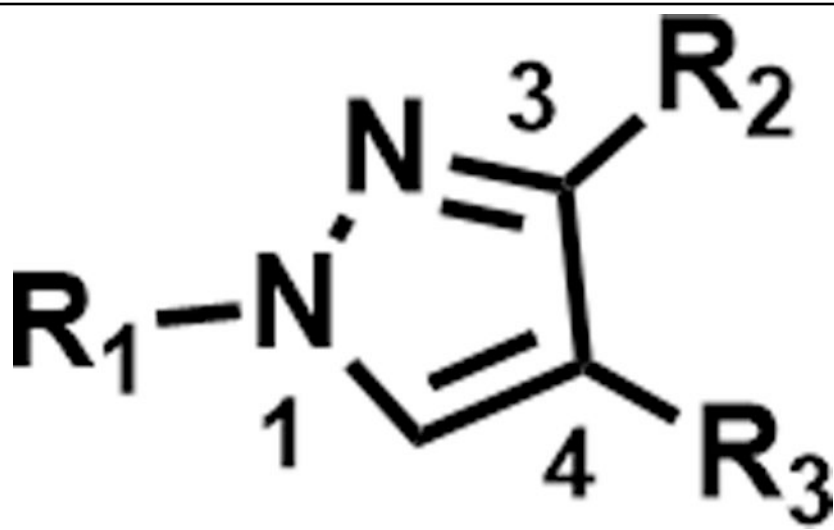
				
Compound Number	X	R <sub>2</sub>	MIC (μM)	Solubility (μM)
18	Br		20	196
19	Br		9.4	60
20	Br		9.4	200
21	Br		>50	196
22	Br		50	200
23	Br		12.5	<5

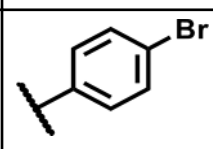
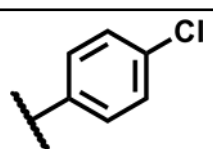
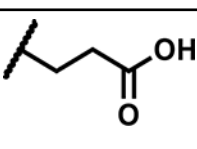
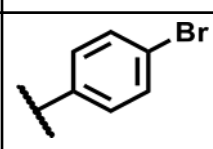
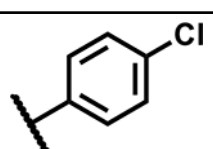
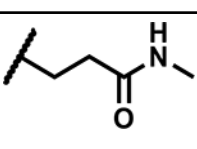
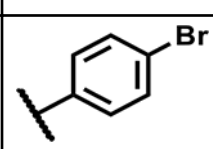
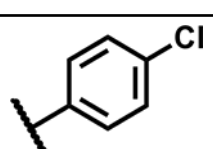
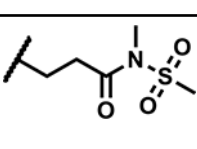
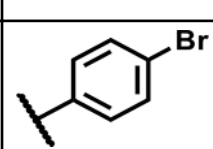
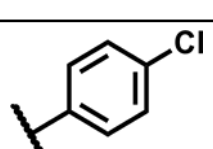
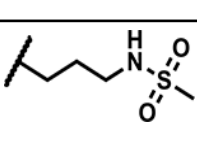
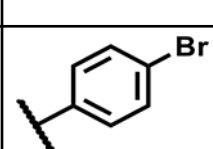
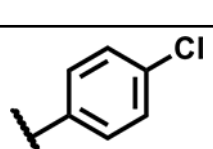
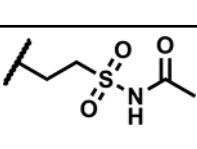


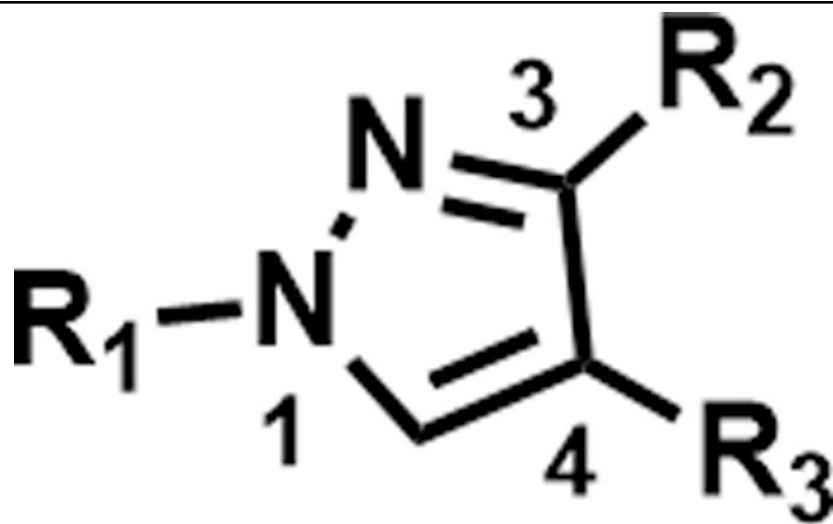
Compound Number	X	R <sub>2</sub>	MIC (μM)	Solubility (μM)
24	Br		25	160
25	Br		>50	200

MIC – were measured in Middlebrook 7H9/Glu/BSA/Tyloxapol media; Solubility – aqueous solubility at pH 7.

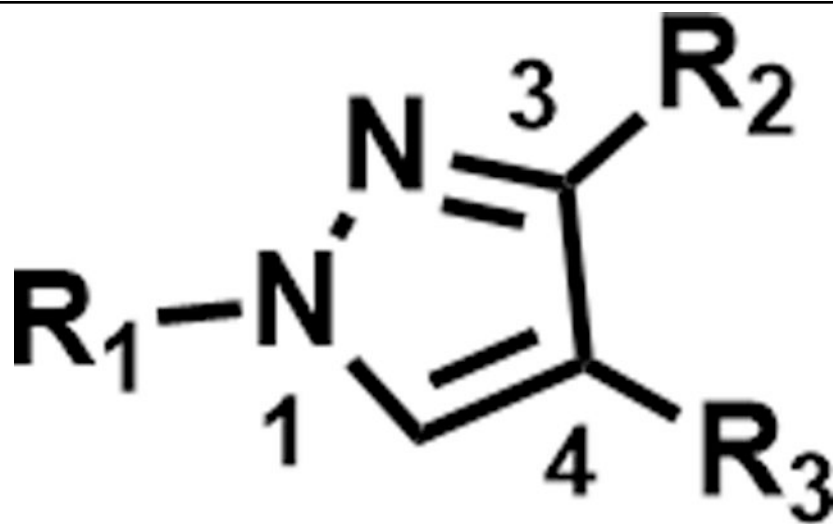
Table 4.

SAR at C4 *N*-sulfonylpropanamide


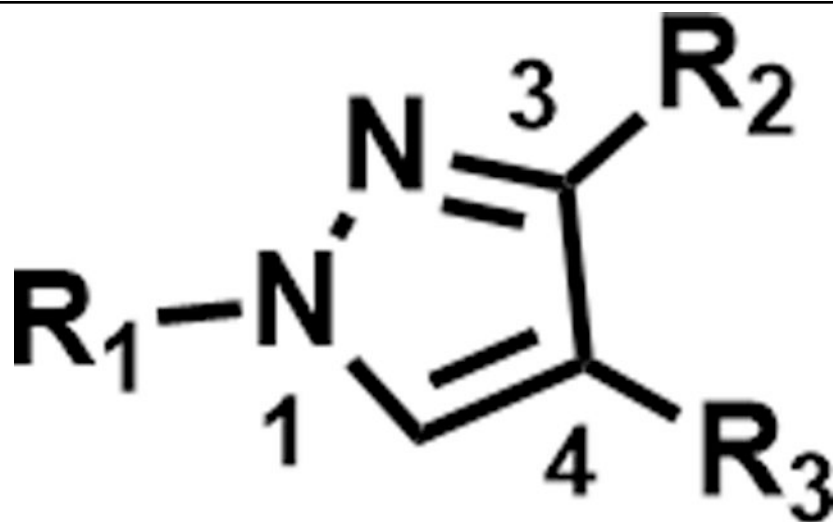
Compound Number	R <sub>1</sub>	R <sub>2</sub>	R <sub>3</sub>	MIC (μM)	Solubility (μM)
26				>50	155
27				>50	<5
28				>50	<5
29				>50	<5
30				>50	165



Compound Number	R <sub>1</sub>	R <sub>2</sub>	R <sub>3</sub>	MIC (μM)	Solubility (μM)
31				>50	200
32				37	135
33				12.5	10
34				>50	5
35				6.25	ND



Compound Number	R <sub>1</sub>	R <sub>2</sub>	R <sub>3</sub>	MIC (μM)	Solubility (μM)
36				>50	190
37				50	170
38				4.7	90
39				1.2	185
40				19	200

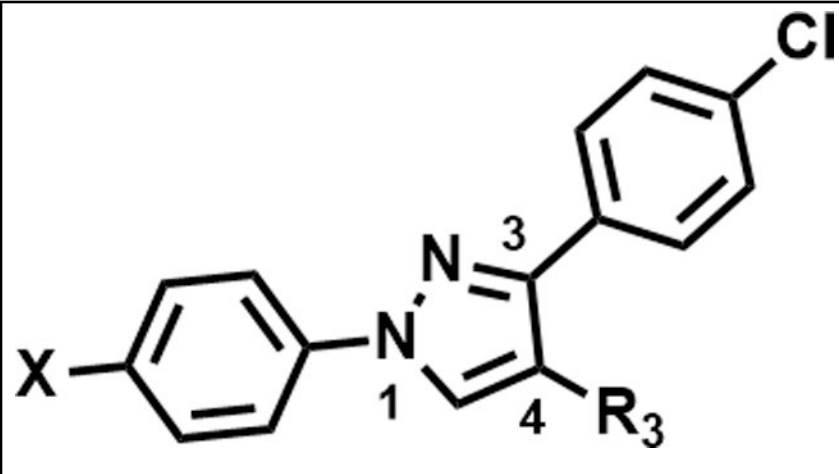


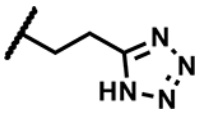
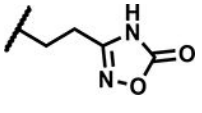
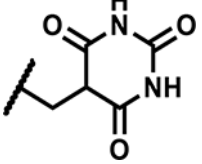
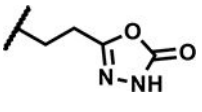
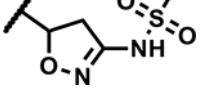
Compound Number	R <sub>1</sub>	R <sub>2</sub>	R <sub>3</sub>	MIC (μM)	Solubility (μM)
41				12.5	155
42				1.2	195
43				1.56	150
44				3.13	<5
45				12.5	ND

MIC – were measured in Middlebrook 7H9/Glu/BSA/Tyloxapol media; Solubility – aqueous solubility at pH 7.

Table 5.

Heterocycles at C4



Compound Number	X	R3	MIC (μM)	Solubility (μM)
46	Br		>50	150
47	Br		50	<5
48	Cl		>50	200
49	Br		19	<5
50	Cl		25	175

MIC –were measured in Middlebrook 7H9/Glu/BSA/Tyloxapol media at day 14; Solubility – aqueous solubility at pH 7.

**Table 6.**

SAR at pyrazole core

Compound Number	Structure	MIC ( $\mu\text{M}$ )	Solubility ( $\mu\text{M}$ )
51		6.25	200
52		5.5	195
53		37	135
54		>50	200
55		>50	170
56		37	200
57		19	90
58		0.15	25

MIC – were measured in Middlebrook 7H9/Glu/BSA/Tyloxapol media; Solubility – aqueous solubility at pH 7.



**Table 7.**MICs against isogenic single-drug resistant mutant strains of *Mtb*

<i>Mtb</i> Strain	MIC ( $\mu$ M)						
	1	8	43	58	RIF	INH	ETH
H37RvMA	4	4	0.5	0.24	0.002	7.8	15.6
<i>cyd</i>	4	4	0.5	0.12	0.005		
QcrB <sup>A317T</sup>	4	4	0.5	0.12	0.005		
MmpL3 <sup>G253E</sup>	4	4	1	0.24	0.005		
MmpL3 <sup>G758A</sup>	2	2	1	0.5	0.004		
DprE1 <sup>Y314C</sup>	3	4	2	0.24	0.005		
DprE1 <sup>P116S</sup>	0.5	0.5	0.12	0.12	0.002		
DprE1 <sup>T314H</sup>	0.5	0.5	0.12	0.12	0.002		
InhA-OE	0.4	0.24	<0.12	<0.13	0.001	31.2	
KatG <sup>T198A</sup>	15.6	15.6	4	1	0.003	>62.5	>125
EthA <sup>C253R</sup>	8	8	2	0.5	0.002	7.8	>125

InhA-OE: InhA overexpressor (H37Rv-LP:*fabG1/inhA-c-15t*); RIF: Rifampicin; INH: Isoniazid; ETH: Ethionamide

**Table 8.**MICs of compound **16** against clinical *Mtb* isolates

<i>Mtb</i> Isolate	Resistant Profiles	MIC of Compound 16 ( $\mu\text{M}$ ) <sup>a</sup>
H37RvMa	Susceptible	15
S2371	Susceptible	30
S1125	Susceptible	15–30
MD55	MDR: INH; RMP; EMB; PZA; SM	60 <sup>b</sup>
MD96	XDR: INH; RIF; AM; KM; CAP; OFLX; EMB; ETH; PZA; SM	30 <sup>b</sup>
R88	INH Mono-Resistant	30 <sup>b</sup>
R296	MDR: INH; RIF; EMB; ETH	60 <sup>b</sup>
R3027	RIF Mono-Resistant	60 <sup>b</sup>

<sup>a</sup>: MIC were determined by MIGIT method

<sup>b</sup>: Values within 4-fold of MICs against drug-susceptible isolate are considered sensitive to the test compound; INH: Isoniazid; RIF: Rifampicin; AM: Amikacin; KM: Kanamycin; CAP: Capreomycin; OFLX: Ofloxacin; EMB: Ethambutol; ETH: Ethionamide; PZA: Pyrazinamide; SM: Streptomycin.

**Table 9.**In vitro and *in vivo* DMPK parameters<sup>a</sup>

Compound	TPSA	LogD	Microsomal clearance H/R/M % remaining	Human PPB <i>fu</i>	<i>t</i> <sub>1/2</sub> terminal (h)	V <sub>d</sub> (L/kg)	CL <sub>b</sub> (mL/min/ kg)	CL <sub>u</sub> (mL/min/kg)	AUC <sub>0-t</sub> (min.μmol/L)
<b>1</b>	81.1	2.4	90/74/71	0.004	2.0	0.2	1.18	295	3527
<b>8</b>	81.1	2.0	98/>99/87	0.023	3.6	1.2	2.56	111	4883
<b>10</b>	93.9	1.87	94/98/94	0.036	3.0	8.7	67.4	1872	134
<b>16</b>	93.9	0.93	85/94/79	0.009	1.3	nd	> 200	>20000	15
<b>17</b>	93.9	0.84	37/95/94	0.022	1.7	28.1	178	8091	31
<b>20</b>	90.3	0.55	86/83/77	0.07	2.3	29.3	145	2071	31
<b>38</b>	93.9	0.98	88/82/85	0.015	1.1	nd	> 200	>20000	8.7
<b>40</b>	93.9	1.06	>99/92/96	0.01	0.9	nd	> 200	>20000	21
<b>43</b>	106	0.81	99/98/91	0.041	2.0	nd	> 200	>4878	29
<b>45</b>	103.2	2.73	97/97/98	0.03	5.8	nd	> 200	>20000	22
<b>51</b>	81.1	2.1	>99/87/91	0.01	3.6	1.0	3.13	313	1359
<b>58</b>	101.6	0.36	98/87/85	0.007	nd	nd	> 200	>20000	20

<sup>a</sup>: *in vivo* mouse PK parameters calculated from non-compartmental analysis of intravenous dosing at 2 mg/kg; TPSA: total polar surface area; H/R/M: Human/Rat/Mouse; PPB: Plasma protein binding; *fu*: Fraction unbound; V<sub>d</sub>: Volume of distribution; CL<sub>b</sub>: Total body clearance determined from whole blood; CL<sub>u</sub>: Unbound blood clearance determined from CL<sub>b</sub> and plasma protein binding (assuming blood to plasma ratio of 1). AUC: Area under the curve; nd: not determined.